JOURNAL
OF
GEOMAGNETISM
AND
GEOELECTRICITY

VOL. IV NO. 1

SOCIETY
OF
TERRESTRIAL MAGNETISM AND ELECTRICITY
OF
JAPAN

APRIL 1952
KYOTO

JOURNAL OF GEOMAGNETISM AND GEOELECTRICITY

EDITORIAL COMMITTEE

Honorary Member: A. TANAKADATE
(Tokyo)

Chairman : M. HASEGAWA
(Kyoto University)

Y. HAGIHARA
(Tokyo Astronomical Observatory)

K. MAEDA
(Electrical Communication Laboratory)

H. HATAKEYAMA
(Central Meteorological Observatory)

N. MIYABE
(Geographic Survey Institute)

S. IMAMITI
(Magnetic Observatory)

T. NAGATA
(Tokyo University)

Y. KATO
(Tohoku University)

H. UYEDA
(Central Radio Wave Observatory)

EDITORIAL OFFICERS: M. OTA and S. MATSUSHITA (Kyoto University)

EDITORIAL OFFICE: Society of Terrestrial Magnetism and Electricity of Japan,
Geophysical Institute, Kyoto University, Japan

The fields of interest of this quarterly Journal are as follows:

Terrestrial Magnetism	Aurora and Night Sky
Atmospheric Electricity	The Ozone Layer
The Ionosphere	Physical States of the Upper Atmosphere
Radio Wave Propagation	Solar Phenomena relating to the above Subjects
Cosmic Rays	Electricity within the Earth

The text should be written in English, German or French. The price is provisionally set as 180 yen per copy subject to change. We hope to exchange this Journal with periodical publications of any kind in the field of natural science.

The Editors

An Effect of the Atmospheric Electric Field upon the Observation of Ions in the Atmosphere

By G. ISHIKAWA, M. KADENA and M. KITAMURA

Meteorological Research Institute, Tokyo

Abstract

In the observation of ions in the atmosphere, we must consider that the observed values should differ from those in the free atmosphere owing to the deformation of the atmospheric electric field caused by the existence of the building, within which the observing instruments are settled. Therefore, comparison among the observed values at various positions would be meaningless, without taking account of such an effect of the electric field.

In this paper, we tried to find the suitable position of the aperture for drawing the air into the building in a few simple cases, so that the consideration of such an effect may be dispensed with.

1. *The case of plane ground*

First we treat of the stationary state of ionization on the plane ground, which we consider as the standard case. Assuming that a uniform electric field is directed downward vertically, that only small ions exist, that the rate of ion production q is constant, and that the loss of ions is only due to the recombination process, then such assumptions do not substantially affect our problem, and so the following expressions may be deduced,

$$\frac{\partial n^+}{\partial t} = q - \alpha n^+ n^- - \operatorname{div} n^+ \boldsymbol{V}^+ \tag{1.1}$$

$$\frac{\partial n^-}{\partial t} = q - \alpha n^- n^+ - \operatorname{div} n^- \boldsymbol{V}^- \tag{1.2}$$

and for simplicity,

$$\boldsymbol{V}^+ = -\boldsymbol{V}^- = k\boldsymbol{E} \tag{1.3}$$

where,

$n^+(n^-)$ is the number density of positive (negative) small ions

$\boldsymbol{V}^+(\boldsymbol{V}^-)$, the velocity of positive (negative) small ions

q, the rate of production of small ions

α, the recombination coefficient for small ions of both signs

k, the mobility of small ions

and $\boldsymbol{E}$ is the electric field intensity.

Assuming the stationary state and taking the smallness of the space charge into consideration, we get from the above three expressions,

$$q-\alpha n^+n^-+kE\frac{dn^+}{dz}=0 \tag{1.4}$$

$$q-\alpha n^-n^+-kE\frac{dn^-}{dz}=0 \tag{1.5}$$

from these equations, we easily obtain

$$n^++n^-=n=\text{constant (independent of } z \text{ and } kE) \tag{1.6}$$

from (1.4) and (1.6), making $E\to 0$

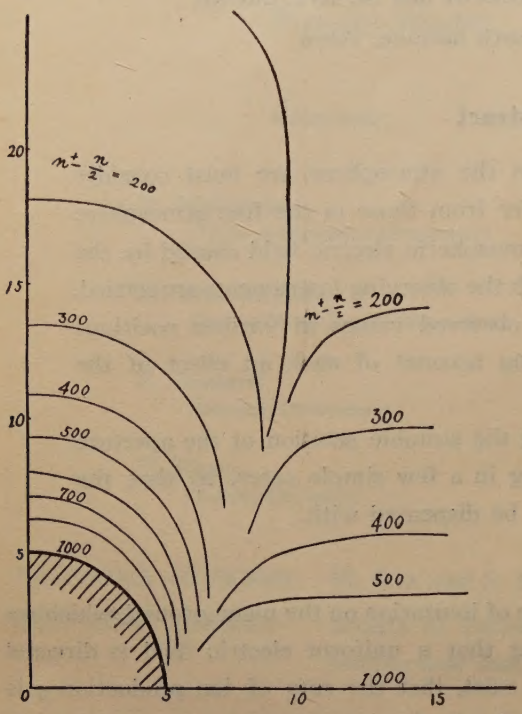


Fig. 1 Semi-spherical building in a vertical electric field. θ_0 is a position where $|E|=E$ is satisfied.

$$n^+(n-n^+)=\frac{q}{\alpha} \quad \text{and} \quad n^+=n^-=\frac{n}{2} \tag{1.7}$$

$$\text{so,} \qquad \frac{n}{2}=\sqrt{q/\alpha}$$

substituting (1.7) into (1.4), we have,

$$(n^+-\sqrt{q/\alpha})^2+\frac{kE}{\alpha}\frac{dn^+}{dz}=0 \tag{1.8}$$

from this equation,

$$n^+=\sqrt{q/\alpha}+\frac{kE}{\alpha z+c} \tag{1.9}$$

Similarly,

$$n^-=\sqrt{q/\alpha}-\frac{kE}{\alpha z+c} \tag{1.9'}$$

where c is the arbitrary integration constant.

Taking account of boundary conditions $(n^-)_{z=0}=0$, $(n^+)_{z=0}=n$, c is easily determined, with which the expressions (1.9) and (1.9′) are written as follows,

$$n^+=\sqrt{q/\alpha}+\frac{kE}{\alpha}\left\{z+\frac{kE}{\sqrt{\alpha q}}\right\}^{-1} \tag{1.10}$$

$$n^-=\sqrt{q/\alpha}-\frac{kE}{\alpha}\left\{z+\frac{kE}{\sqrt{\alpha q}}\right\}^{-1} \tag{1.10'}$$

2. *The case of two-dimensional spherical boundary*

What we have to deal with being the stationary state for this case, the following expressions similar to (1.4) and (1.5) are deduced,

$$q-\alpha n^+n^-=kE\cdot\nabla n^+ \tag{2.1}$$

$$q-\alpha n^-n^+=-kE\cdot\nabla n^- \tag{2.2}$$

In the same manner with the previous section, we have

$$n^++n^-=n=\text{constant}, \qquad \frac{n}{2}=\sqrt{q/\alpha} \tag{2.3}$$

and

$$q-\alpha n^+(n-n^+)=\alpha(n^+-\sqrt{q/\alpha})^2 \tag{2.4}$$

Now, putting

$$T=\frac{k}{\alpha(n^+-\sqrt{q/\alpha})} \tag{2.5}$$

we get from (2.1), (2.4) and (2·5) the following eqution,

$$\boldsymbol{E}\cdot\nabla T=-1 \tag{2.6}$$

If, $E_x=E_y=0$, $E_z=-E$ at infinity,

$$E_r=-E\left(1+\frac{a^2}{r^2}\right)\sin\theta \tag{2.7}$$

$$E_\theta=-E\left(1-\frac{a^2}{r^2}\right)\cos\theta \tag{2.8}$$

where, E_i and a are the i component of the electric field and the radius of the sphere respectively.

From (2.6), (2.7) and (2.8), we have

$$\frac{r^2}{(r^2+a^2)\sin\theta}\,dr=\frac{r^3}{(r^2-a^2)\cos\theta}\,d\theta=E\,dT \tag{2.9}$$

the solution for (2.9) is

$$ET(r,\theta)=\int_b^r f(r,C_1)\,dr+ET(b,\theta_1) \tag{2.10}$$

where,

$$f(r,c_1)=\left\{\left(1+\frac{a^2}{r^2}\right)^2-\frac{c_1^2}{r^2}\right\}^{-\frac{1}{2}} \tag{2.11}$$

$$c_1=\frac{b^2+a^2}{b}\cos\theta_1 \tag{212}$$

b and θ_1 are the values of r and θ at the boundary, and the value of θ on the left side of the equation (2.10) is to be determined by the following equation after carrying out the integration,

$$\theta=\cos^{-1}\left\{\frac{r(b^2+a^2)}{b(r^2+a^2)}\cos\theta_1\right\} \tag{2.13}$$

Since the elliptic integral $\int_b^r f(r,c_1)\,dr$ is a little troublesome, we have integrated numerically. The result is shown in Fig. 2, where the following values are used,

$a=8\pi ek$ (assume $k^+=k^-$)

$n=2\times10^3$/cc

$k=1\dfrac{\text{cm/sec.}}{\text{volt/cm}}$

$E=1$volt/cm

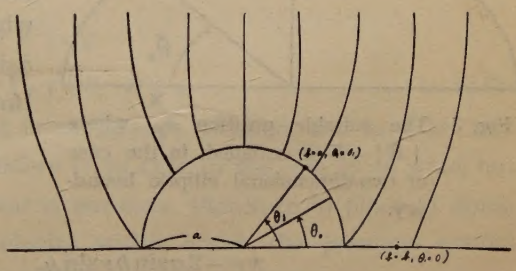


Fig. 2 Equi-ion density line around a two dimensional semi-sphere.

We shall next get the position at which the distribution of ions is similar to those near the plane ground. There may be the same distribution of ions as that on the plane ground near a position on the boundary of the building, on which the same electric field as that on the plane ground exists. In order to get such a position, we have only to find the position on the boundary at which the relation of $|\boldsymbol{E}|=E$ is satisfied, considering that the size of the building is large, and that the effect of the wind is now neglected. The substitution of this relation gives the following result,

$$2E\sin\theta=E \quad \text{or} \quad \theta_0=30^\circ$$

Therefore, in the case of a semi-circular cylinder-shaped building, the effect of the deformation of the electric field due to the building need not be taken into account, if the aperture is set at the position whose angle of elevation in 30 degrees.

3. *Two-dimensional elliptic boundary*

3. A Transversal case

Since the three cases to be stated below are based on the same idea as the case of two-dimensional sphere, we shall omit detailed descriptions. We take the elliptic co-ordinate system in which the surfaces $\nu=$constant and $\mu=$constant show the equi-elliptic surface and equi-hyperbolic surface respectively. Taking the surface, $\nu=\nu_0$, as boundary and $E\nu$, $E\mu$ as the ν and μ component of the electric field respectively, then

$$E_\nu=-\frac{E(e^{\nu}+e^{2\nu_0-\nu})}{2\sqrt{\cosh^2\nu-\cos^2\mu}}\sin\mu \tag{3.1}$$

$$E_\mu=-\frac{E(e^{\nu}-e^{2\nu_0-\nu})}{2\sqrt{\cosh^2\nu-\cos^2\mu}}\cos\mu \tag{3.2}$$

here, ν and μ are connected with the rectangular co-orninates as follows

$$x=2a\cosh\nu\cos\mu, \qquad y=2a\sinh\nu\sin\mu \tag{3.3}$$

The position thus obtained on the boundary at which $|\boldsymbol{E}|=E$ is satisfied is as follows

$$\frac{e\nu_0}{\sqrt{\cosh^2\nu-\cos^2\mu}}\sin\mu=1$$

or

$$\sin\mu=\frac{\cosh^2\nu_0-1}{e^{2\nu_0}-1} \tag{3.4}$$

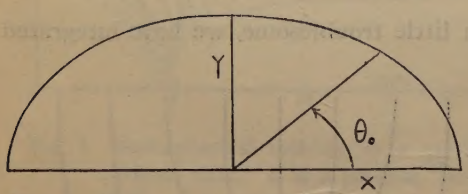


Fig. 3 The suitable position θ_0, where $|\boldsymbol{E}|=E$ is satisfied, in the case of two-dimensional elliptic boundary.

from this and (3.3)

$$\theta_0=\tan^{-1}\left(\frac{y}{x}\right)=\tan^{-1}\left(\frac{Y^2}{X\sqrt{Y^2+2XY}}\right) \tag{3.5}$$

where X and Y are the long and the short axis of the ellipsoidal boundary respectively. Now taking $Y/X=2/3$, then

$$\theta_0=18°30'$$

3. B Vertical case

Similarly to the previous subsection,

$$x=-2a\sinh\nu\sin\mu, \qquad y=2a\cosh\nu\cos\mu \tag{3.6}$$

$$E_\nu=-\frac{E(e^{\nu}+e^{2\nu_0-\nu})}{2\sqrt{\cosh^2\nu-\cos^2\mu}}\cos\mu \tag{3.7}$$

$$E_\mu=+\frac{E(e^{\nu}-e^{2\nu_0-\nu})}{2\sqrt{\cosh^2\nu-\cos^2\mu}}\sin\mu \tag{3.8}$$

The position on the boundary, at which $|\boldsymbol{E}|=E$ is satisfied, is as follows,

$$\frac{e\nu_0}{\sqrt{\cosh^2\nu_0-\cos^2\mu}}=1 \quad \text{or} \quad \cos^2\mu=\frac{\cosh^2\nu_0}{e^{2\nu_0}+1} \tag{3.9}$$

from this and (3.6)

$$\theta_0=\tan^{-1}\left(\frac{X^2}{Y\sqrt{X^2+2XY}}\right)$$

for example, taking $Y/X=2/3$,

$$\theta_0 \fallingdotseq 44°50'$$

4. *The case of three-dimensional spherical boundary*

With the usual polar co-ordinate system, we write the electric field as follows;

$$E_r = E\cos\theta + 2E\frac{a^3}{r^3}\cos\theta \tag{4.1}$$

$$E_\theta = -E\sin\theta + E\frac{a^3}{r^3}\sin\theta \tag{4.2}$$

By the same process as in previous subsections, we easily find,

$$\theta_0 = \sin^{-1}\frac{1}{3} \fallingdotseq 19°28'$$

5. *Summary*

The suitable observing position, θ_0, dispensing with the correction, as shown above, is aproximately determined by the geometric shape of the building and independently of k and $\boldsymbol{E}$. In the case of a square shaped boundary, the calculation of $\boldsymbol{E}$ is difficult, but nevertheless, if we set the aperture for drawing the air on the position, where $|\boldsymbol{E}| = E$ is satisfied, the observed value needs no correction, by the same consideration as above.

Though we have discussed so far the case of no wind, we shall, finally, add the consideration of the effect of the wind.

In this case, the expression of $\boldsymbol{V}^+$ and $\boldsymbol{V}^-$ becomes as follows

$$\left.\begin{aligned} \boldsymbol{V}^+ &= k\boldsymbol{E}+\boldsymbol{V}_0 \\ \boldsymbol{V}^- &= -k\boldsymbol{E}+\boldsymbol{V}_0 \end{aligned}\right\} \tag{5.1}$$

where $\boldsymbol{V}_0$ is the wind velocity. And assume that $\operatorname{div}\boldsymbol{V}_0=0$ is satisfied for simplicity.

From (1.1), (1.2) and at stationary state,

$$\operatorname{div}(n^+\boldsymbol{V}^+ - n^-\boldsymbol{V}^-)=0$$

from this,
$$k\boldsymbol{E}\cdot\nabla(n^+ + n^-) = \boldsymbol{V}_0\cdot\nabla(n^+ - n^-) \tag{5.2}$$

Therefore, the relation of $n^+ + n^- =$ constant is not always satisfied, and so it is clear that the distribution of ions in this case differs from that in the case of no wind, but in the windy case, to get an exact solution is not easy, therefore in place of doing so, we shall show the limit of the wind velocity within which the previous results may be used. Considering the effect of the wind,

$$\operatorname{div} n^-\boldsymbol{V}^- = -k\boldsymbol{E}\cdot\nabla n^- + \boldsymbol{V}_0\cdot\nabla\cdot n^- = -kE_\nu\frac{\partial n^-}{\partial\gamma} + V_0\frac{\partial n^-}{\partial\tau}$$

ν and τ show the direction of normal and parallel to the boundary respectively, and E_ν, V_0 are the perpendicular and parallel components to the boundary of $\boldsymbol{E}$ and $\boldsymbol{V}_0$. From the previous results, only ions near the boundary contribute to the observed values. For example, we consider a two-dimensional sphere. At the boundary, the above equation is written as follows,

$$\operatorname{div} n^-\boldsymbol{V}^- = -kE_\nu\frac{\partial n^-}{\partial\gamma} + \frac{V_0}{a}\frac{\partial n^-}{\partial\theta} \tag{5.3}$$

In this expression, if the first term is far larger than the second the effect of the wind may be neglected,
namely,

$$\left| -kE_r \frac{\partial n^-}{\partial r} \right|_{r \fallingdotseq a} \gg \left| \frac{V_0}{a} \frac{\partial n^-}{\partial \theta} \right|_{r \fallingdotseq a} \tag{5.4}$$

It must be noted that the value at the boundary must not be used in calculation, since the observed ions are not only those on the boundary but rather their space average value near the boundary. The distance from the boundary determining the region for the average depends on the velocity of the inhaled air and the mobility of ions. But, here, in order to know the state roughly, we take the approximate value of n^- at the unit distance from the boundary for the above inequality.
Then we have,

$$| V_0 | \ll 0.4\, a \text{ cm/sec.}$$

where a is the value measured in meter.

For example, if $a=5$ meters, the right side of the above is 2 m/sec. So, at a wind velocity less than the order of 1 m/sec., the results obtained in the previous sections may be approximately valid. Rigourous treatment in the case of strong wind will be performed in future.

We should like to express our, hearty thanks to Dr. Hatakeyama, Director of Meteorological Research Institute, for his kind suggestion in this work.

A Theory of Diurnal Magnetic Variations in Equatorial Regions and Conductivity of the Ionosphere *E* Region

By Motokazu HIRONO

Geophysical Institute, Kyoto University

Abstract

In two previous papers, I suggested that the electrical conductivity in E-W direction of the *E* region in a narrow belt along the magnetic equator is much greater than in the other latitudes, on account of a polarization field produced by the Hall Current, provided that λ is much less than 10. And that this high conductivity will cause enhanced diurnal magnetic variations near the magnetic equator.

In this paper, I discuss this theory further in detail. A dynamo theory for the *E* region with anisotropic conductivity, which is linked by highly conductive lines of magnetic force to the *F* region, is examined. A case that the *E* layer only makes a tidal oscillation, which produces observed lunar diurnal current system, is calculated. It is found that, in middle latitudes, the induced polarization field in E-W direction by the Hall Current is greater than that by the direct current, and the vertical drift of the *F*2 layer by this polarization field seems to be adequate for the observed *F*2 lunar variation. According to the present theory, conductivity of the *E* region at the magnetic equator decreases with increase of the main magnetic field, and the distribution of range of magnetic variations along the magnetic equator reported by Egedal, seems to support this relation.

1. *Introduction*

In the course of statistical researches of Sq field of terrestrial magnetism in middle and low latitudes, it is noticed that the range of diurnal magnetic variations at Huancayo near the magnetic equator (Dip 2.°3 N) is much greater than at other stations. Whether there are other such places than Huancayo, is a matter of great interest. For the purpose

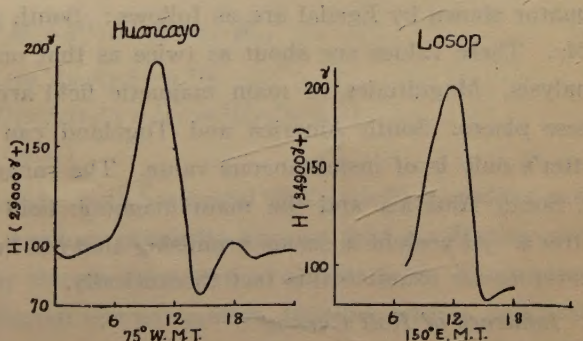


Fig. 1 Diurnal Variation of Magnetic Horizontal Intensity. Mean Values: Losop Feb. 12-15, Huancayo Feb. 11-14 (1934). (After S. Hayami and H. Higashinaka)

of studying solar eclipse of Feb. 14, 1934, Prof. S. Hayami and H. Higashinaka [1] made magnetic observations at Losop Island (6°53′ N, 152°44′ E, Dip 1°45′ N) from Feb. 12 to Feb. 15, which were reported by Prof. M. Hasegawa [3]. In Figure 1 mean H variations are reproduced for Losop (Feb. 12–15) and Huancayo (Feb. 11–14).

Mean ΔH of these are 133γ (instantaneous) for Losop and 138γ (hourly mean) for Huancayo. M. Hasegawa and M. Ota [2], made detailed analysis of the Sq field for the II polar year data and concluded that a line of maximum diurnal magnetic variation (in place of which we write MS line in the following) is supposed, and lies nearly along the magnetic equator (dip zero line). A.T. Price [4] suggests, using the above mentioned data, that this line has some deviation from the magnetic equator. But according to Hasegawa's opinion, it is dangerous to decide this deviation from the above data, because observations near the magnetic equator have been very few, and direct observations in this region will be able to decide an exact deviation.

J. Egedal [5] showed the ranges for 1948–50 near the equator, his results are reproduced in Fig. 2 in which ratios of the ranges to that of Huancayo are shown for South America and India.

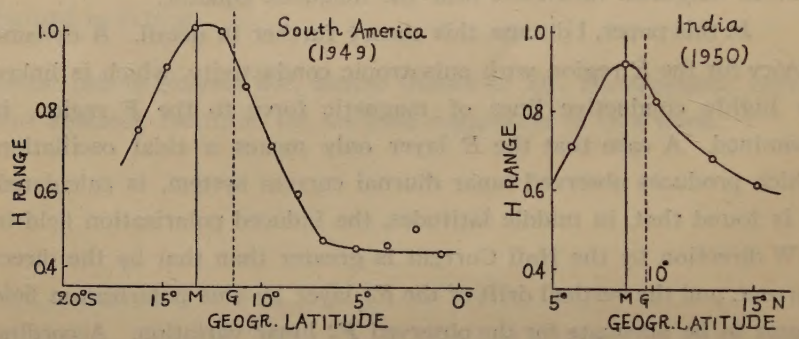


Fig. 2 Comparative Ranges of H refered to Huancayo (After A.A. Giesecke and J. Egedal)
M: Magnetic Equator, G: Geomagnetic Equator (dipole equator)

From these results it is supposed that MS line in the Far East and in the Pacific seems to lie very closely on the magnetic equator. Mean ranges of H at the magnetic equator shown by Egedal are as follows: South America 116γ, India 106γ, Togoland 124γ. These values are about as twice as that on the equator obtained by harmonic analysis. Magnitudes of main magnetic field are 0.3Γ, 0.38Γ, 0.32Γ respectively for these places. South America and Togoland can hardly be compared because the latter's only is of instantaneous value. The range at India seems to be smaller than at South America and the main magnetic field of the former is greater than the latter's. At present it seems promising that MS line agrees with the magnetic equator, therefore we examine this fact theoretically.

2. *Influence of Hall Current*

In two previous papers [6] and [7], hereafter refered to as I and II respectively, we made preliminary calculations on the influence of the Hall Current (in place of which we write H.C. in the following) to the electrical conductivity of the ionosphere.

The present paper describes a further examination of the problem.

To discuss conductivity in the ionosphere, it is necessary to consider a mixture of four gases--neutral molecules, positive ions, negative ions, and electrons. These are distinguished respectively by suffixes a, $+$, $-$ and e, and ions are denoted by i. The mass, charge (in e.m.u.), velocity, number density of r th molecules are denoted by m_r, e_r, $\boldsymbol{c}_r$, n_r, and charge of an electron is specially denoted by $-e$. The number density, temperature of the gas as a whole are n and T. The mass velocity $\boldsymbol{c}_0$ is defined by

$$\boldsymbol{c}_0=\sum_r n_r m_r \overline{\boldsymbol{c}_r}/\sum_r n_r m_r, \tag{1}$$

and the peculiar velocity $\boldsymbol{C}_r$ is defined by $\boldsymbol{C}_r=\boldsymbol{c}_r-\boldsymbol{c}_0$. The gas as a whole is supposed to be almost electrically neutral;

thus

$$\sum_r n_r e_r \simeq 0. \tag{2}$$

The electric current density $\boldsymbol{J}$ can be expressed in the form

$$\boldsymbol{J}=\sum_r n_r e_r \overline{\boldsymbol{c}_r}=\sum_r n_r e_r(\boldsymbol{c}_0+\overline{\boldsymbol{C}_r})=\sum_r n_r e_r \overline{\boldsymbol{C}_r} \tag{3}$$

D.R. Bates [8] suggests that $n_-/n_e \equiv \lambda \ll 1$ in the E and F region. But this value in the E region leaves some doubt, because reactions concerning molecular oxygen is not yet clear. T.G. Cowling [9], discussed the absorption of radio waves and suggested that $\lambda \ll 50$ in the E region. According to Cowling, when λ is not much greater than unity or when $n_a/n_+ > 5\times 10^7$, the diffusion velocity $\overline{\boldsymbol{C}_r}$ can be expressed by the same form as for the free path method. In the ionosphere, the above conditions will be satisfied. When we discuss Sq current system, according to I § 1, we get the next relation as a good approximation,

$$\begin{cases} \overline{\boldsymbol{C}_r}=(e_r/m_r)\{\nu_r/(\nu_r^2+\omega_r^2)\}\boldsymbol{E}_\perp-(1/H)\{\omega_r^2/(\nu_r^2+\omega_r^2)\}\boldsymbol{h}\times\boldsymbol{E}+(e_r/m_r\nu_r)\boldsymbol{E}_\parallel \ (r\neq a) \\ \overline{\boldsymbol{C}_a}\simeq 0 \end{cases} \tag{4}$$

where $\boldsymbol{E}=\boldsymbol{E}^{(s)}+\boldsymbol{c}_0\times\boldsymbol{H}$ (in e.m.u.), $\boldsymbol{E}^{(s)}$ = electrostatic field, $\boldsymbol{H}$ = the earth's main magnetic field, $\boldsymbol{h}$ = unit vector in the direction of $\boldsymbol{H}$, $1/\nu_r=m_r D_r/kT$, D_r = Diffusion coefficient between r th molecule and neutral molecule. $\omega_r=e_r H/m_r$, $\boldsymbol{E}_\perp$, $\boldsymbol{E}_\parallel$ = Component vectors of $\boldsymbol{E}$ perpendicular and parallel to the magnetic field. using (2), (3) and (4) we get

$$\boldsymbol{J}=\sigma^I\boldsymbol{E}_\perp+\sigma^{II}\cdot\boldsymbol{h}\times\boldsymbol{E}+\sigma_\parallel\cdot\boldsymbol{E}_\parallel, \tag{5}$$

where

$$\begin{cases} \sigma^I=e^2\sum_r(n_r/m_r)\{\nu_r/(\nu_r^2+\omega_r^2)\} \\ \sigma^{II}=(n_e e/H)\{\omega_e^2/(\nu_e^2+\omega_e^2)-\omega_i^2/(\nu_i^2+\omega_i^2)\} \\ \sigma_\parallel=e^2\sum_r(n_r/m_r\nu_r) \end{cases}$$

According to the dynamo theory, both horizontal tidal velocity $\boldsymbol{c}_0$ and the earth's magnetic field $\boldsymbol{H}$ in the ionosphere, produce primarily dynamo field $\boldsymbol{c}_0\times\boldsymbol{H}$, the vertical component of which is canceled by the resulting vertical electric field. The horizontal component of which produces a diurnal current system, together with a polarization field due to the resulting charge distribution. Near the E region, when $\lambda \ll 1$ is satisfied, it is shown that $\sigma^I \sim 3\times 10^{-21} n_e$, $\sigma^{II} \sim 5\times 10^{-20} n_e$, therefore $\sigma^{II}/\sigma^I \sim 10$. Electric field produces not only a direct current, but also considerable H.C, which is shown by the

second term of (5), therefore the dynamo theory may have to contain σ^{II} and differ from those of A. Schuster and S. Chapman. When λ is not smaller than 1, σ^{II}/σ^{I} becomes about $1/(2\lambda+1)$ times the above mentioned value, since σ^{I} becomes about $(2\lambda+1)$ times and σ^{II} is not increased. When $\lambda \gg 1$ is satisfied, we can neglect H.C., and even when λ is small σ^{II}/σ^{I} rapidly decreases upward from the E region. At first we treat the case that the axes of rotation and magnetism of the earth coincide.

Suppose that a uniform electric field is impressed in E-W direction near the equator, then H.C. tends to flow vertically, but it cannot flow counteracted by a resulting polarization field; and as a resultant conductivity in E-W direction, we get

$$\sigma^{III}=\sigma^{I}\{1+(\sigma^{II}/\sigma^{I})^{2}\}, \tag{6}$$

which is shown in II, (10).

In this case positive and negative charges can move vertically by the same amount in the same direction. Let rectangular axis O-xyz be taken, so placed that ox, oy, and oz are directed to the south, east, and upward respectively and unit vectors in the direction of ox, oy, and oz be $\boldsymbol{i}$, $\boldsymbol{j}$ and $\boldsymbol{k}$ respectively.

We treat first an ionosphere near the equator. Suppose that the layer is initially confined between $z=a_1$ and $z=a_2$ $(a_1>a_2)$, electron density depends on z only and is mainly controled by electron production and recombination, and that λ is uniform, gas density distribution is the same as the real E region. This treatment will be adequate, since the thickness of the E region is several ten kms and the diurnal electric field is supposed to be approximately uniform over several thousand kms. The charge density is denoted by ρ, the electric field is supposed to be perpendicular to the magnetic field, then we have the next equation in this layer

$$\boldsymbol{J}=\sigma^{I}\cdot\boldsymbol{E}+\sigma^{II}\boldsymbol{h}\times\boldsymbol{E}, \tag{7}$$

$$\nabla\cdot\boldsymbol{E}=4\pi c^{2}\rho, \tag{8}$$

$$\partial\rho/\partial t=-\nabla\cdot\boldsymbol{J} \tag{9}$$

Suppose that constant electric field E_0 is impressed in oy direction from the time $t=0$, then H.C. produces polarization field $E_z\boldsymbol{k}$, and we get $\boldsymbol{E}=E_0\boldsymbol{j}+E_z\boldsymbol{k}$. Substituting this for $\boldsymbol{E}$ in (7) we have

$$J_y=\sigma^{I}\cdot E_0+\sigma^{II}\cdot E_z,\quad J_z=\sigma^{I}\cdot E_z-\sigma^{II}\cdot E_0. \tag{10}$$

As electron production and recombination are so rapid that variations of σ^{I} and σ^{II} with current are negligible, the next equation is obtained $\partial J_z/\partial t=\sigma^{I}\cdot(\partial E_z/\partial t)$, on the other hand $\partial E_z/\partial t=-4\pi c^{2}J_z$, therefore $\partial J_z/\partial t=-4\pi c^{2}\sigma^{I}J_z(a_2<z<a_1)$ $\therefore J_z=J_{z0}e^{-t/\alpha}$, $\alpha=1/4\pi c^{2}\sigma^{I}$. As in the E region we have $\sigma^{I}\sim 3\times10^{-21}n_e$ for gas density $n=10^{13}$ and $\lambda\ll1$, therefore $\alpha\sim3\times10^{-2}/n_e$. For so low an electron density $n_e=1$, follows $\alpha\sim3\times10^{-2}$sec. For $n_e=10^{5}$ we have $\alpha=3\times10^{-7}$sec, but it is doubtful that we can treat the processes in such a short time by our present theory, since $1/\nu_i\sim2\times10^{-4}$sec. at $n=10^{13}$. Nevertheless we can deduce that J_z rapidly tends to zero after a time, say 2×10^{-3}sec. When λ is not smaller than 1, α becomes about $1/(2\lambda+1)$ times the above value. Thus almost instantaneously, a steady state is attained and the relation

$$J_z=\sigma^{I}E_z-\sigma^{II}E_0=0 \tag{11}$$

holds at any height of the layer. At the same time from (10) $J_y=\sigma^{I}\{1+(\sigma^{II}/\sigma^{I})^{2}\}\cdot E_0$, therefore the conductivity of equation (6) is obtained at any height. Using equation

(7) we get $\nabla\cdot\boldsymbol{J}=\sigma^I\nabla\cdot\boldsymbol{E}+\sigma^{II}\cdot\nabla(\boldsymbol{h}\times\boldsymbol{E})+\nabla\sigma^I\cdot\boldsymbol{E}+\nabla\sigma^{II}\cdot\boldsymbol{h}\times\boldsymbol{E}$. Writing $\sigma^I=n_e\cdot\sigma_\nu{}^I$, $\sigma^{II}=n_e\cdot\sigma_\nu{}^{II}$, and considering equ. (8) and $\nabla\cdot(\boldsymbol{h}\times\boldsymbol{E})=-\partial E_0/\partial z=0$ we get the following equation

$$-\partial\rho/\partial t=4\pi c^2\cdot\sigma^I\cdot\rho+n_e\{E_z(\partial\sigma_\nu{}^I/\partial z)-E_0(\partial\sigma_\nu{}^I/\partial z)\}+(\sigma_\nu{}^I\cdot E_z-\sigma_\nu{}^{II}\cdot E_0)\cdot\partial n_e/\partial z \quad (12)$$

At the steady state, it follows from this equation that,

$$\rho=\left(E_0\cdot\frac{\partial}{\partial z}\sigma_\nu{}^{II}-E_z\cdot\frac{\partial}{\partial z}\sigma_\nu{}^I\right)/4\pi c^2\cdot\sigma_\nu{}^I \quad (13)$$

This quantity depends on gas density and not on the electron density. In the E region we infer that

$$\sigma_\nu{}^I\sim(2\lambda+1)\cdot1.76\times10^{-8}/n,$$
$$\sigma_\nu{}^{II}\sim(1/H)1.59\times10^{-20}(1-1.12\times10^{23}/n^2).$$

We take local scale height as 10km, then $\partial n/\partial z=10^{-6}\cdot n$. We have from (13), using these relation, $\rho=-E_0\cdot9.03\times10^{-28}$ for $\lambda\ll1$, and $n=10^{13}$. When solar tidal oscillations in this layer are l_s times as great as those at the ground, we get $E_0\sim3.7l_s$ (e.m.u.) on the equator according to a later section, then we get

$$\Delta n_e=\rho/(-e)=2.17\times10^{-7}\cdot l_s.$$

As l_s is estimated to be the order of 10^2, Δn_e is very small. Thus we can see how well the condition of electrical neutrality (2) is satisfied. When $\lambda\lessdot1$ holds, we can also see the the same result. Next denote the total charge in a vertical column, which has a unit cross section on a plane $z=z_1$ and is confined in the range $z\leqq z_1$, by q, then we have at $z=z_1$, $E_z=4\pi c^2q$. At the steady state, using (11) we obtain $q=(1/4\pi c^2)(\sigma^{II}/\sigma^I)E_0=5.8\times10^{-21}\,l_s$ for $n=10^{13}$ at $z=z_1$. Let the length of the column be d, then from the above relation it follows that $d\cdot\Delta n_e=q/e=3.65\times10$ for $l_s=10^2$. For the value $d\sim10$km, we get $\Delta n_e\sim3.65\times10^{-5}$.

If gas density in this layer is uniform, space charge distribution ρ in the layer vanishes almost instantaneously and E_z arises by a surface charge distribution q. From (11), as the mean value in the E region, we get $\overline{E}_z=6\cdot E_0$ for $\lambda\ll1$.

3. *Conductivity at any Latitudes*

We treat the same the distribution of ionosphere as in the previous section. Here the magnetic field is supposed to be uniform with dip ϕ (constant). When a uniform electric field is impressed in either E-W direction or in N-S direction, we can show that the vertical current vanishes almost instantaneously on account of a vertical polarization field, but in this steady state, a vertical mass movement of the layer remains. When a uniform electric field $(E_x\boldsymbol{i}+E_y\boldsymbol{j})$ is impressed, in the steady state we have

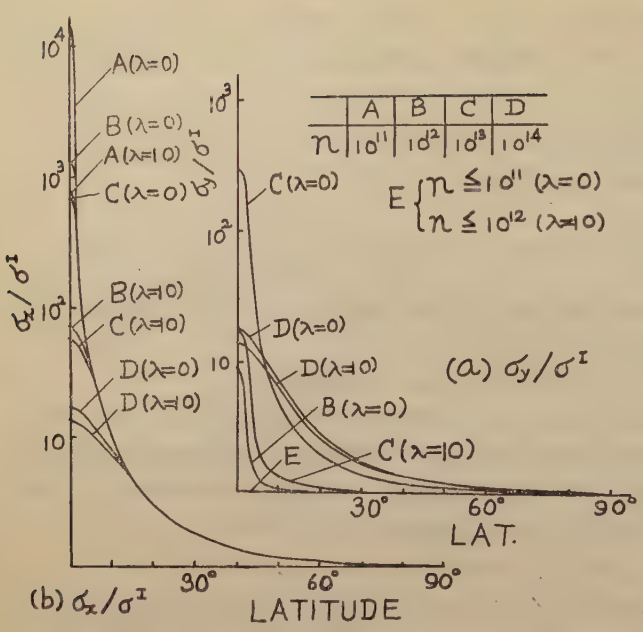
$$J_x=\sigma_xE_x+\sigma_{xy}E_y,\qquad J_y=\sigma_{yx}E_x+\sigma_yE_y \quad (14)$$

$$E_z=\{\sigma^{II}\cos\phi\cdot E_y-(\sigma_{/\!/}-\sigma^I)\sin\phi\cos\phi\cdot E_x\}/(\sigma_{/\!/}\cdot\sin^2\phi+\sigma^I\cdot\cos^2\phi) \quad (15)$$

where

$$\left.\begin{aligned}&\sigma_x=\sigma^I/\{\sin^2\phi+(\sigma^I/\sigma_{/\!/})\cos^2\phi\}\\&\sigma_{xy}=\sigma^{II}\sin\phi/\{\sin^2\phi+(\sigma^I/\sigma_{/\!/})\cos^2\phi\}\\&\sigma_{yx}=-\sigma_{xy}\\&\sigma_y=\sigma^I+(\sigma^{II}\cos\phi)^2/(\sigma^I\cos^2\phi+\sigma_{/\!/}\sin^2\phi)\end{aligned}\right\} \quad (16)$$

The values of σ_x and σ_y were already discussed in I, § 3 but σ_{xy} in I, (17) is not valid



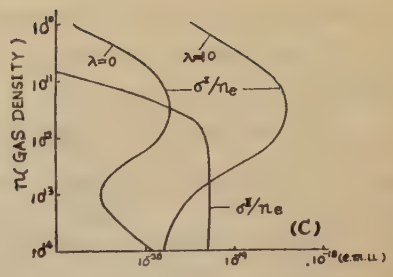


Fig. 3. The calculated values of (a) σ_y/σ^I, (b) σ_x/σ^I with latitude, and (c) σ^I/n_e, σ^{II}/n_e with gas density.

since it does not take the vertical polarization field into consideration. The values of σ_y/σ^I, σ_x/σ^I are illustrated with latitude in Figs 3 (a) and (b). σ^I/n_e and σ^{II}/n_e with gas density are shown in Fig. 3 (c). Here we use the value by Ferraro [10] for D_i with molecular weight 20 for ion and 25 for neutral molecule. D_e is refered to gas kinetic value, and H is taken to be 0.3 (e.m.u.) Therefore, we take the values $\nu_e = 1.31\times10^{-8}\cdot n$, $\nu_i = 4.36\times10^{-10}\cdot n$. At middle latitudes $\sigma_x \sim \sigma^I$ and $\sigma_y \sim \sigma^I$. The above equations will be approximately valid, since both the magnetic field and diurnal electric field are supposed to be fairly uniform over far greater horizontal distance than the thickness of the ionosphere. To discuss the electrical conductivity of the E region in higher latitudes than about 7.°5, it is necessary to consider E and $F1$ regions, which make tidal oscillations with air velocity $u_1\boldsymbol{i}+v_1\boldsymbol{j}$ and $u_2\boldsymbol{i}+v_2\boldsymbol{j}$ respectively.

Let current density integrated with height in E and $F1$ regions be $\boldsymbol{I}_1$ and $\boldsymbol{I}_2$, horizontal electrostatic field be $\boldsymbol{E}_1 = X_1\boldsymbol{i}+Y_1\boldsymbol{j}$ and $\boldsymbol{E}_2 = X_2\boldsymbol{i}+Y_2\boldsymbol{j}$. Then we get the following equations, for the E region,

$$\begin{cases} I_{1x} = \alpha_x(v_1H_z+X_1)+\alpha_{xy}(-u_1H_z+Y_1) \\ I_{1y} = \alpha_{yx}(v_1H_z+X_1)+\alpha_y(-u_1H_z+Y_1) \end{cases} \tag{17}$$

for the $F1$ region,

$$\begin{cases} I_{2x} = \beta_x(v_2H_z+X_2) \\ I_{2y} = \beta_y(-u_2H_z+Y_2) \end{cases} \tag{18}$$

where $\alpha_r = \int_E \sigma_r dh$ $(r = x, xy, yx, y)$, $\beta_r = \int_{F1} \sigma_r dh$, β_{xy}, β_{yx} are effectively zero. As in the usual dynamo theory, the relation $\nabla\cdot\boldsymbol{J}\simeq 0$ can be readily seen here.

If we take the F region in place of the $F1$, the values of β_r will be a little increased.

An ideal case that these two layers are electromagnetically independent, was first raised by Dr. K. Maeda [11].

But we think that interactions of these layers are important. At present it is most probable that the Sq current flows mainly in the E region. We imagine the following model for Sq field in the daytime. In the northern hemisphere, anticlockwise electric field (dynamo field plus electrostatic field) of a whirl shape will be present. Direct curect will flow along this field as shown by I. Fig. 4. Horizontal component of H.C. will flow in such a way as to concentrate negative charges to the focus of the whirl. This polarization will, however, be considerably dissipated by direct current in the F region in the opposite direction to the lower horizontal H.C.; since in higher latitudes than about 7.°5, as shown in II, the E region is connected by highly conductive lines of magnetic force to the F region. Therefore the effective conductivity of the E region in these latitudes will be much less than that at the magnetic equator.

In the following we suppose that $\lambda \ll 1$, E and $F1$ layers are thin spherical shells with the above mentioned conductivities, and their distances are so small that they can be represented by a common radius a in mathematical treatment.

Let E and $F1$ layers be Chapman layers with local scale height 10km and 30km, gas densities at these centers be 6×10^{12} and 10^{11}, and maximum electron densities 10^5/cc and 2.5×10^5/cc. For this model, we obtain a distribution of $\sigma_{/\!/}$ with height. Between E and $F1$ layers we obtain by a numerical calculation, $1/\overline{(1/\sigma_{/\!/})}=7.95\times10^{-13}$ (e.m.u.) which is very great compared with the values at respective centers, $\sigma^I(E)=4.4\times10^{-16}$ and $\sigma^I(F1)=3.58\times10^{-15}$. Therefore we can show that E and $F1$ regions are connected by highly conductive lines of force in middle latitudes. But vertical current will be very small. Here we assume that Sq current system is nearly horizontal, i.e. $J_z \ll \sqrt{J_x^2+J_y^2}$. Considering the relation $\sigma_{/\!/} \gg \sigma^I, \sigma^{II}$, equation (15) can be reduced to

$$E_z \simeq -\cot\phi \cdot E_x. \tag{19}$$

On the other hand, as the third term of equation (5) can be written as

$$\sigma_{/\!/}\boldsymbol{E}_{/\!/}=\sigma_{/\!/}(-E_x\cos\phi-E_z\sin\phi)\boldsymbol{h}$$

equation (19) implies that $\boldsymbol{E}_{/\!/}$ is very small. Therefore, if $\boldsymbol{E}_z$ deviates a little from the value of (15), current flows almost in the direction of lines of magnetic field, and the above assumption is violated. Thus equation (15) and consequently (14), (16), (17) and (18) hold with good approximation, in this case. As the relation between E_x, E_y, and E_z in the equation (15) is linear, we can divide E_z into two parts; the one produced by the horizontal dynamo field, and the other produced by the horizontal electrostatic field. These sets satisfy the equation (15) respectively. In the following we treat the latter set. Let a vertical square *abcd* be taken, as shown in Fig. 4, so placed that *ab* and *cd* are horizontal and situated at the center of E and $F1$ region, and in the direction of electric field in a practical sense, and that this square is fixed to the earth. Horizontal electrostatic fields on *ab* and *cd* be E_h and E'_h, which are measured positively in the direction of $\vec{ab}$, upward vertical component of electrostatic fields on *bc* and *ad* be E_z and E'_z.

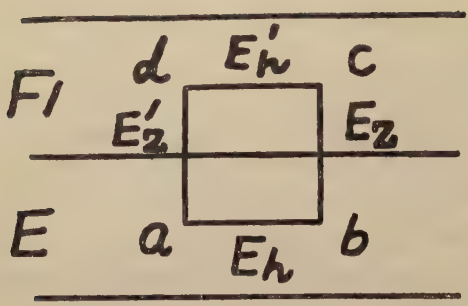


Fig. 4

As $\oint \boldsymbol{E}ds=0$ around $abcd$, we obtain the following equation

$$\bar{E}_h-\bar{E}'_h=\bar{E}'_z-\bar{E}_z, \tag{20}$$

where bar denotes mean value on each side of the square.

Let a length of one side be L, which is of the order of 10^7cm. Direction cosine of $\vec{ab}$ be $(l, m, 0)$, then differential coefficient in the direction of ab can be written, using equation (19) as

$$dE_z/ds=-l(E_x\cdot\partial\cot\phi/a\partial\theta+\cot\phi\cdot\partial E_x/a\partial\theta)-m(\cot\phi\cdot\partial E_x/a\sin\theta\partial\lambda)$$

We deduce, from the observed results, that

$$\partial E_x/a\partial\theta\sim E_x/a,\quad \partial E_x/a\sin\theta\partial\lambda\sim E_x/a$$

Therefore
$$\partial E_z/\partial s=-(E_x/a)[l\{2/\sin^2\phi(1+3\cos^2\theta)+\cot\phi\}+m\cot\phi] \tag{21}$$

Under the assumption that horizontal electric field in every region is of the same order of magnitude as that at the center of the region, and considering that $\bar{E}'_z-\bar{E}_z \simeq(d\bar{E}_z/ds)L$, we can make the following estimation. In higher latitudes than 20°,

$$|\bar{E}_h-\bar{E}'_h|\leqq\{|\bar{E}_h|+|\bar{E}'_h|\}\cdot\left|l\left(l\cdot\frac{1}{30}+m\cdot\frac{1}{80}\right)\right|$$

$$\therefore\quad |\bar{E}_h-\bar{E}'_h|\ll|\bar{E}_h|+|\bar{E}'_h|.$$

This relation holds approximately near 7.°5 but does not hold in lower latitudes if $\vec{ab}$ is in the N-S direction. Therefore in higher latitudes than 7.°5 we can take $\bar{E}_h=\bar{E}'_h$ as a first approximation. Thus we write $X_1=X_2=X$, $Y_1=Y_2=Y$ in (17) and (18).

The above result will be approximately valid for E and F region. For such a uniform current system as Sq, difference of the height of current sheet, of 100km, gives negligible difference to the variation of terrestrial magnetism at the ground. Therefore, Sq is produced by $\boldsymbol{I}=\boldsymbol{I}_1+\boldsymbol{I}_2$ in a good approximation. We can, further, treat in such a way that $\partial I_x/a\partial\theta+\partial I_y/a\sin\theta\partial\lambda=0$, to be derived from $\nabla\cdot\boldsymbol{J}=0$, considering $J_z=0$ on the outer surfaces of the combined layer.

Then the following two cases are examined.

(I) F region is at rest i.e. $u_2=v_2=0$ and E region makes tidal oscillations. We write $\boldsymbol{I}=I_x\boldsymbol{i}+I_y\boldsymbol{j}$, ($I_z\ll I_x$, I_y), and from (17) and (18), get

$$\begin{cases} I_x=a_x(v_1H_z+X)+a_{xy}(-u_1H_z+Y)+\beta_xX \\ I_x=a_{yx}(v_1H_z+X)+a_y(-u_1H_z+Y)+\beta_yY \end{cases} \tag{22}$$

$X\boldsymbol{i}+Y\boldsymbol{j}$ can be derived from a potential S, i.e. $X=-\partial S/a\partial\theta$, $Y=-\partial S/a\sin\theta\partial\lambda$. Substituting these values in (22) and by the eiimination of S, we have

$$\frac{\partial}{\partial\lambda}\left(\frac{1}{K_x}I_x\right)-\frac{\partial}{\partial\lambda}\left(\frac{1}{K_{xy}}I_y\right)-\frac{\partial}{\partial\theta}\left(\frac{\sin\theta}{K_y}I_y\right)+\frac{\partial}{\partial\theta}\left(\frac{\sin\theta}{K_{yx}}I_x\right)$$
$$=\frac{\partial}{\partial\lambda}\{H_z(M_1u_1+M_2v_1)\}+\frac{\partial}{\partial\theta}\{H_z\sin\theta(M_3u_1+M_4v_1)\} \tag{23}$$

where

$$K_x=(\alpha_x+\beta_x)+\frac{\alpha_{xy}^2}{\alpha_y+\beta_y},\qquad K_y=(\alpha_y+\beta_y)+\frac{\alpha_{xy}^2}{\alpha_x+\beta_x},$$
$$K_{xy}=\alpha_{xy}+(\alpha_x+\beta_x)(\alpha_y+\beta_y)/\alpha_{xy},\qquad K_{yx}=-K_{xy},$$
$$M_1=-(\beta_y\cdot\alpha_{xy})/\Delta,\qquad M_2=\{\alpha_x(\alpha_y+\beta_y)+\alpha_{xy}^2\}/\Delta,$$
$$M_3=\{(\alpha_x+\beta_x)\alpha_y+\alpha_{xy}^2\}/\Delta,\qquad M_4=(\beta_x\cdot\alpha_{xy})/\Delta,$$
$$\text{with}\qquad \Delta=(\alpha_x+\beta_x)(\alpha_y+\beta_y)+\alpha_{xy}^2$$

Here we assume that electron density is constant at the same altitude. At the latitudes, here concerned, we get the following values approximately

$$K_x=K_1/\sin^2\phi,\qquad K_y=K_1=(\alpha^I+\beta^I)+(\alpha^{II})^2/(\alpha^I+\beta^I)$$
$$K_{xy}=K_0/\sin\phi,\qquad K_0=\alpha^{II}+(\alpha^I+\beta^I)^2/\alpha^{II}$$

where $\alpha^I=\int_E\sigma^I dh$ etc. (ϕ=Dip).

$$M_1=-\gamma_1/\sin\phi,\quad M_2=\gamma_2,\quad M_3=\gamma_2,\quad M_4=\gamma_1/\sin\phi,$$

where $\gamma_1=\beta^I\cdot\alpha^{II}/G,\quad \gamma_2=\{\alpha^I(\alpha^I+\beta^I)+(\alpha^{II})^2\}/G,$

with $G=(\alpha^I+\beta^I)^2+(\alpha^{II})^2$

K_1, K_0, γ_1, γ_2 are independent of λ and θ, if we neglect very slow variations depending on the magnitude of the magnetic field. Let velocity potential of the air be

$$\Psi_\sigma^s=k_\sigma^s P_\sigma^s\sin(\sigma t+\alpha_\sigma^s),\qquad (24)$$

where k_σ^s is taken to be positive, $t=t'+\lambda$ denotes local time, P_m^n denotes associated Legendre function of Neumann.

Then $u_1=\partial\psi_\sigma^s/a\partial\theta,\quad v_1=\partial\psi_\sigma^s/a\sin\theta\partial\lambda.$

We write $H_z=C\cos\theta$ ($C<0$), and the right hand side of equation (23) is reduced to the form,

$$-\frac{1}{a}\cdot C\cdot k_\sigma^s\sin\theta\left\{\frac{\gamma_2(\sigma+2)\sigma}{2\sigma+1}P_{\sigma+1}^\sigma\sin(\sigma t+\alpha_\sigma^s)+\gamma_1\cdot\sigma\Phi(\theta)P_\sigma^\sigma\cos(\sigma t+\alpha_\sigma^s)\right\}\qquad (25)$$

where $\Phi(\theta)=3\cos^2\theta/(1+3\cos^2\theta)\cdot\sin\phi$

We shall treat, mainly the semi-diurnal air velocity ($\sigma=2$). For numerical example, two cases (a), and (b) are considered.

Case (a) $\alpha^I=5\times10^{-9},\quad \alpha^{II}=3\times10^{-8},\quad \beta^I=4\times10^{-8}$ (e.m.u.)

using these values we get

$$K_1=13\alpha^I,\quad K_0=19.5\alpha^I;\quad \gamma_1=0.41,\quad \gamma_2=0.385$$

Case (b) $\alpha^I=5\times10^{-9},\quad \alpha^{II}=3\times10^{-8},\quad \beta^I=1.5\times10^{-8}$

using these values we get

$$K_1=13.6\alpha^I,\quad K_0=8.16\alpha^I;\quad \gamma_1=0.346,\quad \gamma_2=0.77$$

These values of case (a) are obtained in II. If Bates and Massey's [17] estimation of gas density depending on rocket measurements, are correct, then case (b) will be better. At present the effective conductivity of the F layer to the electrostatic field is not yet clear and these examples will give rough order of magnitude to the following calculation.

The values of $\left|\frac{\gamma_2(\sigma+2)\sigma}{2\sigma+1}P_{\sigma+1}^\sigma\right|$ and $\left|\gamma_1\cdot\sigma\cdot\Phi(\theta)P_\sigma^\sigma\right|$, for $\sigma=2$ and case (a), are

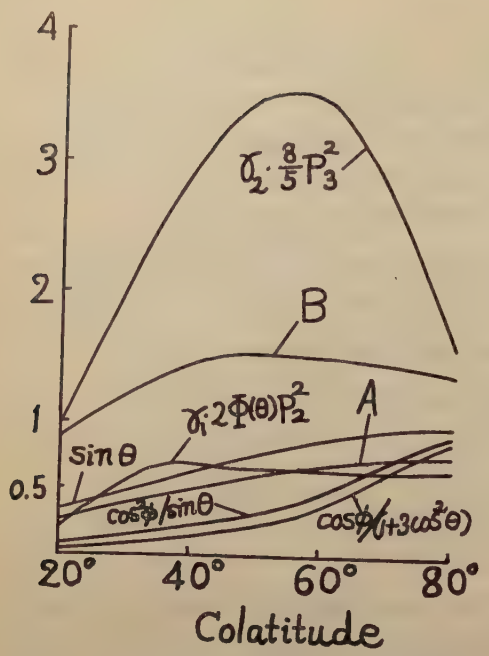


Fig. 5 The Values of $\gamma_2 \cdot (8/5)P_3^2$, $\gamma_1 \cdot 2\Phi(0)P_2^2$; $\sin\theta$, $\cos^2\phi/\sin\theta$, $\cos\phi/(1+3\cos^2\theta)$; and A, B of the equation (38), with colatitude.

shown with colatitude θ, in Fig. 5. As the latter's is much less than the former's, we can neglect the second term of (25), to discuss the order of magnitude. For case (b) we obtain the same result.

Since $\nabla \cdot \boldsymbol{I} = 0$, $\boldsymbol{I}$ can be derived from a current function R, i.e.

$$I_x = \partial R/a\sin\theta\partial\lambda, \quad I_y = -\partial R/a\partial\theta.$$

After substitution, of these values, the left hand side of equ. (23) is reduced to the next form,

$$\frac{1}{aK_1}\left[\left\{\frac{\partial^2 R}{\sin\theta\partial\lambda^2}+\frac{\partial}{\partial\theta}\left(\sin\theta\cdot\frac{\partial R}{\partial\theta}\right)\right\}-\cos^2\phi\cdot\frac{\partial^2 R}{\sin\theta\partial\lambda^2}\right]+\frac{1}{aK_0}\cdot\frac{2\cos\phi}{1+3\cos^2\theta}\cdot\frac{\partial R}{\partial\lambda} \tag{26}$$

Suppose that the current function R, to be determined from (23), is expressed by a tesseral harmonic, $R = r_n^m P_n^m \sin(mt+\alpha_n^m)$. (27)

By substitution of this value, (26) is reduced to the form,

$$\frac{1}{aK_1}\left\{-\sin\theta\cdot n(n+1)r_n^m P_n^m\sin(mt+\alpha_n^m)+\frac{\cos^2\phi}{\sin\theta}\cdot m^2\cdot r_n^m P_n^m\sin(mt+\alpha_n^m)\right\}$$
$$+\frac{1}{aK_0}\cdot\frac{\cos\phi}{1+3\cos^2\theta}\cdot 2m\cdot r_n^m P_n^m\cos(mt+\alpha_n^m) \tag{28}$$

As we are treating semi-diurnal variations, $m=2$, and moreover $n\geqq 3$, since the current must be symmetrical against the equator. The values of $\sin\theta$, $\cos^2\phi/\sin\theta$, $\cos\phi/(1+3\cos^2\theta)$ are shown in Fig. 5 with colatiude. From these results we can eliminate the second term of (28) against the first term. Further, considering $n(n+1)/K_1 \geqq 0.925/a^I$ and $2m/K_0 = 0.205/a^I$ for case (a), we can neglect the third term of (28). Thus (28) can be expressed by the first term neglecting an error of the order of about 30%. For case (b), we can obtain similar results.

Hence equation (23) can be recuced to the equation,

$$\sin\theta\cdot n(n+1)r_n^m P_n^m\cdot\sin(mt+\alpha_n^m) = C\cdot K_e\cdot k_\sigma^\sigma\sin\theta\cdot\frac{(\sigma+2)\sigma}{2\sigma+1}P_{\sigma+1}^\sigma\sin(\sigma t+\alpha_\sigma^\sigma) \tag{29}$$

where $K_e = K_1\cdot\gamma_2$

Therefore, $$R = r_{\sigma+1}^\sigma\cdot P_{\sigma+1}^\sigma\sin(\sigma t+\alpha_\sigma^\sigma) \tag{30}$$

where $$r_{\sigma+1}^\sigma = C\cdot K_e\cdot k_\sigma^\sigma\sigma/(\sigma+1)\cdot(2\sigma+1).$$

On the other hand, when the spherical shell has direct, isotropic, constant conductivity K only, dynamo equations for this case are written as

$$\left.\begin{aligned} v_1 H_z - \frac{\partial S}{a\partial\theta} &= \frac{1}{K}\frac{\partial R}{a\sin\theta\partial\lambda} \\ -u_1 H_z - \frac{\partial S}{a\sin\theta\partial\lambda} &= -\frac{1}{K}\frac{\partial R}{a\partial\theta} \end{aligned}\right\} \tag{31}$$

From these two equations, by eliminating S, and substituting (27) for R, and K_e for K, the same equation as (29) is obtained. Hence K_e is interpreted as an effective conductivity to the dynamo current in these latitudes. K_e is represented as

$$K_e = \alpha^I + (\alpha^{II})^2/(\alpha^I + \beta^I), \tag{32}$$

and $K_e = 5\alpha^I$ for case (a), $K_e = 10\alpha^I$ for case (b).

(II) E and $F1$ regions make tidal oscillations with the same velocity i.e. $u_2 = u_1$, $v_2 = v_1$.

In place of equation (22) we obtain

$$\left\{\begin{aligned} I_x &= (a_x + \beta_x)(v_1 H_z + X) + a_{xy}(-u_1 H_z + Y) \\ I_y &= a_{yx}\cdot(v_1 H_z + X) + (a_y + \beta_y)(-u_1 H_z + Y) \end{aligned}\right. \tag{33}$$

From these equations we have, in place of (23),

$$\frac{\partial}{\partial\lambda}\left(\frac{1}{K_x}I_x\right) - \frac{\partial}{\partial\lambda}\left(\frac{1}{K_{xy}}I_y\right) - \frac{\partial}{\partial\theta}\left(\frac{\sin\theta}{K_y}I_y\right) + \frac{\partial}{\partial\theta}\left(\frac{\sin\theta}{K_{yx}}I_x\right)$$
$$= \frac{\partial}{\partial\lambda}(v_1 H_z) + \frac{\partial}{\partial\theta}(\sin\theta\cdot u_1 H_z) \tag{34}$$

The left hand side of this equation can be reduced in the same way as before, and the right hand side is reduced without any neglection, to the first term of (25), in which 1 is substituted for γ_2. By the same deduction as before, effective conductivity K_1 is obtained. The value of K_1 is $K_1 = K_e + \beta^I$. Therefore, in this case also, effective conductivity of the E layer is considered to be K_e.

4. *Sq current near the Magnetic Equator*

In a narrow belt along line of zero dip of several degrees wide, the equation (19) may not hold, since both current and magnetic fields are nearly horizontal. The σ_{yx} in the equation (14) will not be valid and σ_{yx} in I, (17) might be better and the difference of these values is very great. At present we have not been able to find the best value of σ_{yx}. Thus, we treat this region rather in the same way as in section 2.

In this belt in the E region, we have

$$I_{1x} \simeq a_{//} X_1, \qquad I_{1y} \simeq \alpha^{III}\cdot Y_1$$

where $\alpha^{III} = \int_E \sigma^{III} dh$, $a_{//} = \int_E \sigma_{//} dh$.

In this belt, in the $F1$ region, $I_{2x} \simeq \beta_{//} X_2$, $I_{2y} \simeq \beta^I Y_2$.

By the same way as in middle latitudes, we can show that $Y_1 \simeq Y_2$, but we have $X_1 \neq X_2$. Hence effective conductivity in E-W direction will be $\alpha^{III} + \beta^I$ and that in N-S direction will be a certain average of $a_{//}$ and $\beta_{//}$. The latter will be larger than the former, since $\sigma_{//}$ is much greater than σ^I, σ^{II} and σ^{III}. As the most resistant part is effective to the dynamo current, $\alpha^{III} + \beta^I$ will be the effective conductivity in this belt.

For case (a) $\alpha^{III}+\beta^{I}=45\alpha^{I}$, $(\alpha^{III}+\beta^{I})/K_1=3.5$, $\alpha^{III}/K_e=7.5$

and for case (b) $\alpha^{III}+\beta^{I}=39.6\alpha^{I}$, $(\alpha^{III}+\beta^{I})/K_1=3$, $\alpha^{III}/K_e=3.7$.

For any case, effective conductivity in this belt is greater than 3 times that in middle latitudes. This conductivity will slowly decrease from the equator towards 7.°5 of latitudes. Therefore, to see the outline of the Sq current distribution, we may use the dynamo equation (31) for the following distribution of K, (A) $K=K_L$ (const.) for $0<\theta<\theta_1$ (B) $K=\nu K_L$ for $\theta_1<\theta<\pi-\theta_1$ (C) $K=K_L$ for $\pi-\theta_1<\theta<\pi$, $\theta_1=85°$ is used in this section. From equation (31), by eliminating S we obtain

$$\frac{\partial^2 R}{\sin\theta\partial\lambda^2}+\frac{\partial}{\partial\theta}\left(\sin\theta\cdot\frac{\partial R}{\partial\theta}\right)=aK\left\{\frac{\partial(vH_z)}{\partial\lambda}+\frac{\partial(uH_z\sin\theta)}{\partial\theta}\right\} \tag{35}$$

First, we consider the solution of the equation

$$\frac{\partial^2 R}{\sin\theta\partial\lambda^2}+\frac{\partial}{\partial\theta}\left(\sin\theta\cdot\frac{\partial R}{\partial\theta}\right)=0 \tag{36}$$

Substituting $R=f(\theta)\cdot F(\lambda)$ in the above, we get equations (20) and (21) in II. The solution of (21) in II is denoted by Q_0^M by Hobson [13]. Using his formula, an integral of (36) is expressed as

$$\sum_M\{A_M(1-\mu^2)^{\frac{1}{2}M}/(1-\mu)^M+B_M(1-\mu^2)^{\frac{1}{2}M}/(1+\mu)^M\}(D_M\sin M\lambda+E_M\cos M\lambda), \tag{37}$$

where M is an integer, $\mu=\cos\theta$, and A_M, B_M, D_M, E_M are integrating constants. A general value of the integral of (35) is obtained as the sum of a particular integral of (35) and the above integral. Thus, for semi-diurnal variation we obtain the following solution

(A) $R=B\cdot K_L\{P_3^2(\theta)+C_1q_1(\theta)\}\sin(2t+\alpha)$

(B) $R=B\nu K_L\{P_3^2(\theta)+C_2q_1(\theta)+C_3q_2(\theta)\}\sin(2t+\alpha)$

(C) $R=B\cdot K_L\{P_3^2(\theta)+C_4q_2(\theta)\}\sin(2t+\alpha)$

where $B=(2/15)Ck_2^2$, $q_1(\theta)=(1-\mu)/(1+\mu)$, $q_2(\theta)=(1+\mu)/(1-\mu)$

Considering the continuity of the normal component of the current and the tangential component of the electrostatic field along the boundary between (A), (B) and (B), (C), we determine C_1, C_2, C_3, C_4. Eastward current J_y is obtained by the following equation $J_y=-\partial R/a\partial\theta=J_0(\theta)\sin(2t+\alpha)$, $J_0(\theta)/(-BK_L)$ with colatitude is shown in Fig. 6 (a). Curve A denotes the case $\nu=1$ and curve B the case $\nu=2$ both for $\theta_1=85°$. Amplitude of J is shown in Fig. 6 (b). Thus we can show MS line by the line of maximum amplitude of J. When solar tidal oscillations in the ionosphere are l, times as great as those at the ground, according to Chapman [14], we get $k_2^2\sim 5l_2a$.

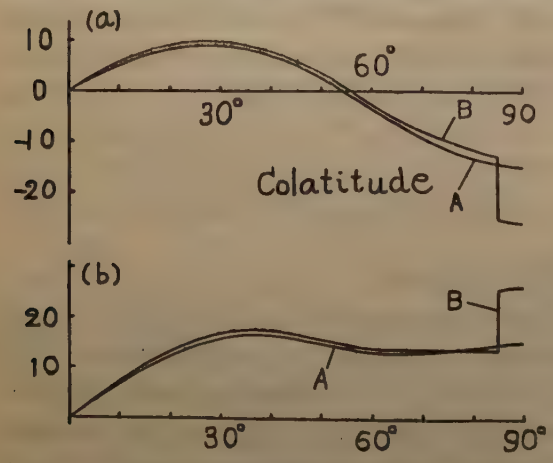


Fig. 6 (a) $J_0(\theta)$, (b) Amplitude of Current Density in unit of $(-2Ck_2^2K_L/15a)$

5. *Vertical Drift Velocity of F2 Layer produced by the Hall Current*

In this section we discuss the case that only E region makes tidal oscillations. In section 3, we showed that $\boldsymbol{E}_1 \simeq \boldsymbol{E}_2$, and this result will be approximately valid for E and F region. Since this conclusion depends upon some assumption and deduction, it is clearly desirable to submit it to a direct test. It has been shown above that when we discuss semi-diurnal variation, in higher latitudes than 7.°5, the current function $R = r_3^2 P_3^2 \sin(2t+\alpha)$, $\alpha = \alpha_3^2$ is a fairly good approximation for the current. From equations (22) and the above value we obtain

$$Y = (1/a)\cdot C\cdot k_2^2 \{A \sin(2t+\alpha) + B \sin(2t+\alpha+90°)\} \tag{38}$$

$$= (1/a)\cdot C\cdot k_2^2 \cdot D \sin(2t+\alpha+\varphi), \tag{39}$$

where
$$A = (K_e/K_1)\{(-2/15)\partial P_3^2/\partial\theta + \cos\theta\cdot\partial P_2^2/\partial\theta\}$$
$$B = (4/3)(K_e/K_0)\sin\phi\cdot P_2^1 + (2/\sin\phi)\cdot P_2^1\cdot(\alpha^{II}/K_1 - \alpha^I/K_0)$$

In $F2$ region the second term of equation (4) is the same for ions and electrons, and a vertical component W of this term represents the vertical drift of this region. Thus, we obtain

$$W = \frac{\cos\phi}{H_0\sqrt{1+3\cos^2\theta}}\cdot Y. \tag{40}$$

D.F. Martyn [15] suggested that main seat of the lunar current is the D region. Later, it was pointed out by Cowling and Borger [16], that conductivity of the D region is too low to be a main seat. The same objection was stressed by Bates and Massey [17]. Though the F region has considerable conductivity, induction drag [9] and kinematic viscosity are very effective in this region. Tidal motion in this region may be very small, from the theoretical point of view. Therefore, it will be possible that lunar main current flows in the E region. Suppose that lunar main current flows in the E region, then $\alpha = -17°$ should be satisfied to agree with Chapman's results for 1905 equinox (14).

If Hall Current is not taken into account, Y is of the same phase as the first term of equation (38), then W is almost downward during 6 hours after lunar transit. While as regards world wide lunar $F2$ variation, except very near the magnetic equator, amplitudes of oscillation of $h'F2$ and $h_{F2}^{\max}$ are about 2~4 km, and maximum height is attained about 6 hours after lunar transit [15]. Therefore alike Martyn's, a conclusion might arise that a reverse lunar currrent flows both in E and F region. But for case (a), since $|B|$ is greater than $|A|$, as shown in Fig. 5, and φ becomes about 70°, therefore upward maximum of W is attained about 7 hours after lunar transit. Hence no contradiction will take place with $F2$ variation, when the E region is the main seat of the current.

When tidal oscillation in the E region is l_L times as great as that at the ground, amplitude of W at $\theta = 60°$ is 0.527 l_L cm/sec. For case (b) a similar result is obtained.

As the observations of lunar E variations are very few and detailed characteristics are not yet clear, we have hesitated to discuss them.

We tentatively suggest that the main seat of the lunar current is the E region.

6. *Variation of Conductivity depending on the Main Magnetic Field and* λ

We shall consider the variation of conductivity depending on main magnetic field and λ. Here we take the value of D_i which was suggested by Tyndall (1938) [18] using observed mobility of N_2^+ and that of D_e which was shown by Huxley (1949) [19]. Molecular weights of ion and neutral molecule are taken to be 26, temperature of the gas to be 300°K. Therefore we take the values $\nu_e = 8.4 \times 10^{-9} \cdot n$, $\nu_i = 5.09 \times 10^{-10} \cdot n$. We represent the E layer at the equator at noon by a Chapman distribution with center at the gas density $n = 10^{13}$ and for local scale height of 10^5cm.

According to examination in section 2, σ^{III} will vary to some extent depending on the magnitude of H, since σ^I varies little with H but σ^{II} varies considerably with H. We calculated conductivity of this layer using equ. (6), by numerical integration for various values of λ and H. S_3 denotes the case $H = 0.3$ and S_4 the case $H = 0.4$ (e.m.u.)

On the other hand we calculate conductivity A of this layer using σ^I and Formula by Appleton [20] for the case $\lambda = 0$, and get the following values $A = A_i + A_e$ where $A_i = n_{e0} \cdot 1.55 \times 10^{-14} H^{-\frac{1}{2}}$, $A_e = n_{e0} \cdot 3.1 \times 10^{-16} H^{-2}$ with n_{e0} the maximum electron density of this layer.

When $\lambda \neq 0$, we assumed that $A = A_e + (2\lambda + 1) A_i$. The ratio S/A with λ is illustrated in Fig. 7 for $H = 0.3$ and 0.4. The ratio S_3/S_4 for various values of λ is shown in Table 1.

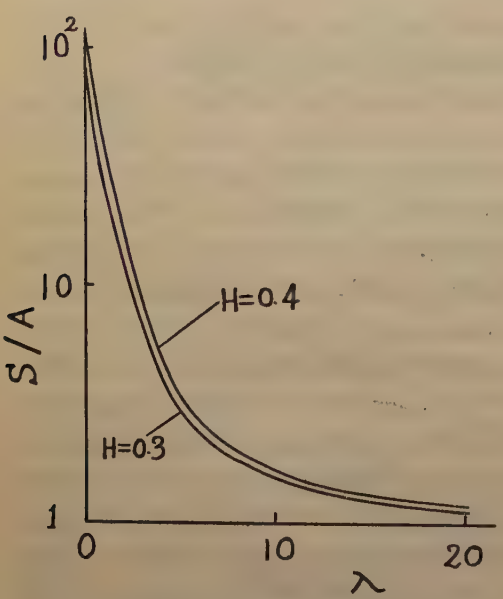


Fig. 7 S/A with the ratio of negative ions to electrons for various values of H.

Table 1

λ	0	10	20
S_3/S_4	1.4	1.27	1.19

The ratio S/A may be a little smaller than curves in Fig. 7, because magnetic and electric fields are not completely uniform. When $\lambda \sim 10$, it can be shown that effective conductivity of the E layer in middle latitudes is approximately equal to A. And moreover, the contribution of the $F1$ layer to the Sq current will be present. Thus to explain observed data with the present theory, λ should be much smaller than 10. According to Table 1, S decreases with increase of H, we imagine that difference of the ranges at Huancayo and at India might be due to this relation.

7. *Concluding Remarks*

In succession to two preliminary work I, II we further examined a theory that enhanced diurnal magnetic variations near the magnetic equator is an effect of high

conductivity in E-W direction due to the polarization field near the E layer produced by Hall Current. The above calculation is made for the case that the axes of rotation and magnetism coincide. In the actual case that the two axes do not coincide and local anomalies are present, MS line will be along the magnetic equator (line of dip zero). If the concentration of the negative ions is effectively zero, the effective conductivity of the E layer in middle latitudes is shown to be some 5 times that obtained by Appleton's formula. It is tentatively suggested that the main seat of the lunar current is the E region, considering the vertical drift of the $F2$ layer, produced by the polarization field due to the Hall Current. According to the present theory conductivity of the E layer decreases with increase of the main magnetic field at the magnetic equator and observed distribution of ranges of diurnal variations reported by Egedal, seems to support this relation.

Moreover this theory is effective only when λ is much smaller than 10. Recent observed results seems to be favourable to the present theory. Further observations near the equators are very desirable.

Acknowledgements

The author wishes to express his thanks to Prof. M. Hasegawa for his continued interest and advice, and to Prof. T. Nagata for his valuable discussions during the progress of this work.

Many thanks are due to Dr. K. Maeda for his criticisms and helpful advice in this work.

References

[1] S. Hayami and H. Higashinaka, J. Shanghai Institute (in Japanese), Sec. I, **3**, 129 (1934).
[2] M. Hasegawa and M. Ota, 'Transactions of Oslo meeting, 1948,' 426 (1950).
[3] M. Hasegawa, 'Transactions of Brussel meeting, 1951' (in the Press).
[4] A.T. Price, J. Geophys. Res., **56**, No. 2, 259 (1951).
[5] J. Egedal, 'Transactions of Brussel meeting, 1951, (in the Press).
[6] M. Hirono, J. Geomag. Geoel. Kyoto, **2**, 1 (1950).
[7] M. Hirono, J. Geomag. Geoel. Kyoto, **2**, 113 (1950).
[8] D.R. Bates and H.S.W. Massey, Proc. Roy. Soc. Lon. **A, 187**, 261 (1946).
[9] T.G. Cowling, Proc. Roy. Soc. Lon. **A, 183**, 453 (1945).
[10] V.C.A. Ferraro, Terr. Mag. Washington D.C., **50**, 215 (1945).
[11] K. Maeda, Read at the meeting of Ionosphere Research Committee, Feb. 29. 1952.
[12] S. Chapman and J. Bartels, 'Geomagnetism II,' 768 (1940).
[13] E.W. Hobson 'The Theory of Spherical and Ellipsoidal Harmonics' 89, Cambridge (1931).
[14] S. Chapman, Phil. Tran. Roy. Soc. Lon., **218**, 1 (1919).
[15] D.F. Martyn, Proc. Roy. Soc. Lon., **A, 194**, 445 (1948).
[16] T.G. Cowling and R. Borger, Nature, Lon. **162**, 143 (1948).
[17] D.R. Bates and H.S.W. Massey, J. Atmos. and Terr. Phys., **2**, 1 (1951).
[18] A.M. Tyndall, Positive Ions, Camb. (1938).
[19] L.G.H. Huxley, A.A. Zaazou, Proc. Roy. Soc. Lon., **199**, 402 (1949).
[20] E.V. Appleton, Proc, Roy. Soc. Lon. **162**, 451 (1937).

(Read Apr. 28, 1952)

Self-Reversal of Thermo-Remanent Magnetism of Igneous Rocks*

By Takesi NAGATA, Seiya UYEDA and Syun-iti AKIMOTO

(Geophysical Institute, Tokyo University)

(Read Oct. 22, 1951 and Apr. 29, 1952)

Abstract

An experimental proof of self-reversal of thermo-remanent magnetization of igneous rocks is obtained. By cooling in a weak magnetic field, some igneous rocks and the ferromagnetic minerals separated from the mother rocks can have the remanent magnetization whose direction is opposite to that of the magnetic field during cooling. The processes of development and decay of the reverse thermo-remanent magnetization by cooling and heating respectively were directly observed (Figs. 11~19) and the characteristics of its appearance were examined. A few possible mechanisms of appearance of this peculiar phenomenon are discussed with reference to Néel's theory.

1. *Introduction*

It has frequently been reported (1), (2), (3) that some igneous rock masses have the remanent magnetism, the direction of which is almost opposite to that of the present geomagnetic force. This phenomenon of reverse remanent magnetism has been found at various localities in the world.

On the other hand, that the remanent magnetism of igneous rocks is usually due to the so-called thermo-remanent magnetism has been experimentally proved by a number of investigators (4), (5), (6) and theoretically treated by L. Néel (7). That is, a mass of igneous rock after cooling in a weak magnetic field from a temperature above the Curie point has generally a relatively strong remanent magnetism, the direction of which is just coincident with that of the magnetic field applied during its cooling.

Since the above-mentioned phenomenon of thermo-remanent magnetism looks like a general characteristics of igneous rocks, several authors (6), (8), (9) tried to conclude that the direction of geomagnetic field at the time when the rock mass of reverse remanent magnetism was cooled down was opposite to that of the present field.

This conclusion seems to be reasonable, so far as we assume that remanent magnetism is the thermo-remanent magnetism, and that the remanent magnetism has been stable during a long time since the ejection or intrusion of the rock-mass.

* Contribution from the Division of Geomagnetism and Geoelectricity, Geophysical Institute, Tokyo University. Series II, No. 32.

However, here is a question: Is there any other process of producing the remanent magnetism of igneous rocks? Or more directly speaking, is there any process of producing the remanent magnetism whose direction is opposite to the applied magnetic field?

L. Néel (10) has recently proposed a few theoretical possibilities of the self-reversal of thermo-remanent magnetism. The present writers have also been attacking the above-mentioned question, experimentally and theoretically. In this preliminary note, the results of experiment of demonstrating the reversal of thermo-remanent magnetism will be reported.

2. *General Description of the Test Sample*

The rock specimen concerned here is a hypersthene hornblende dacite of Mt. Haruna, an extinct volcano in Kwantō District. These dacitic rocks are distributed widely on the north-east slope of Mt. Haruna, and they are of the form of pumice of fairly large size, 40*cm* in their mean diameter.

These dacitic pumices have the natural remanent magnetism of 4.3×10^{-3}*e.m.u.* in average intensity, and its direction is almost opposite to that of the present geomagnetic force, i.e. D=215° I=−14°.

For the purpose of examining in detail the magnetic characteristics refered to its chemical and mineralogical compositions, the ferromagnetic minerals contained in the rock were separated by two different methods. i.e. by means of a magnetic separator and by a panning method. Those mineral grains are the phenocrysts in the mother rocks, being 0.4*mm* in mean diameter. The result of chemical analysis of the ferromagnetic mineral by I. Iwasaki and K. Katsura (11) is given in Table I where the numerals in the righthand side mean the relative amountes of Fe_2O_3, FeO and TiO_2, excluding the other elements.

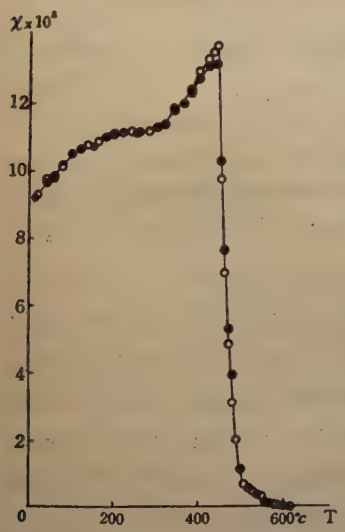


Fig. 1. Change of magntic susceptibility with temperature in at weak field. (*H*= 1.35 *Oe.*)

Table I
Chemical Composition
(HK 51070801 b)

Fe_2O_3	53.15%	57.9%
FeO	31.93	34.7
TiO_2	6.82	7.4
MnO	0.69	—
V_2O_3	0.49	—

The change of magnetic susceptibility of the ferromagnetic mineral in a weak magnetic field was measured by a ballistic method apparatus (12), the result being illustrated in Fig. 1. As will be seen in this figure, the change in susceptibility of the sample with temperature is stepwise, having apparently two Curie points, i.e. 540°C and about 280°C. This result may indicate that the ferromagnetic minerals concerned here are composed mainly of two kinds of ferromagnetic substances, one being, of course, magnetite, while the other might be a combined state of Fe_2O_3–FeO–TiO_2.

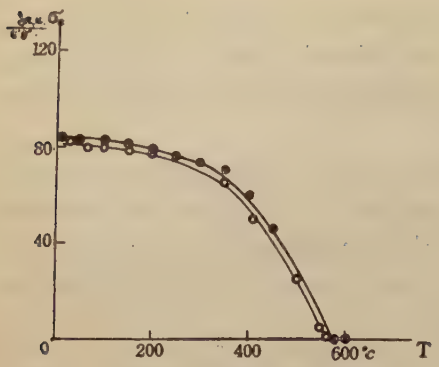


Fig. 2. Change of saturation magnetization with temperature. (H=2000 *Oe.*)

On the other hand, Fig. 2 shows the intensity of saturation magnetization of this mineral in the temperature range from 10°C to 650°C. The magnetization changes with temperature almost in accordance with Curie's Law, where Curie point is about 570°C. It can be said, therefore, that the largest part of the ferromagnetic mineral is magnetite.

3. *Reversal of Thermo-Remanent Magnetism of Rock Sample and Separated Ferromagnetic Minerals.*

The procedure of magnetic field cooling of test sample were carried out under these different conditions: i.e. (a) in a non-inductive and non-magnetic vacuum furnace, (b) in a non-inductive and non-magnetic N_2-furnace, where the pressure of N_2 gas was kept around 780*mm*Hg, and (c) in a non-magnetic furnace in the free atmospheric air. The magnetic field in the furnace can be varied with the aid of a Helmholtz's coil.

The test samples of the rock were of the form of a circular cylinder, 10*cm* long and 2*cm* in diameter, while the ferromagnetic grains were put in a cylindrical tube of fuzed silica, 10*cm* long and 6*cm* in its inner diameter.

The thermo-remanent magnetizations (T.R.M.s) produced by cooling down the test sample to the room temperature (10°C) from various temperatures from 300°C to 600°C in magnetic field of 0.5 *Oe.* are shown in Fig. 4. As is shown in this figure, the direction of T.R.M. thus produced are opposite to that of applied magnetic field.

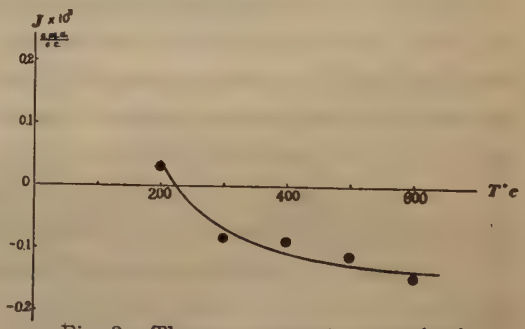


Fig. 3. Thermo-remanent magnetization, $J^{10}_{T,H=0.5}$ of the rock sample.

In the ordinary rock samples or ordinary ferromagnetic minerals, T.R.M. is always "positive," i.e. the direction of T.R.M. is parallel to that of applied magnetic field. Such the ordinary case will be named hereafter "**normal thermo-remanent magnetism**" or shortly "**Normal T.R.M.**" In the case of Eig. 3, however, T.R.M. has a negative value, i.e. the direction of T.R.M. is reversed. So that such the case of T.R.M. will be called "**reverse thermo-remanent**

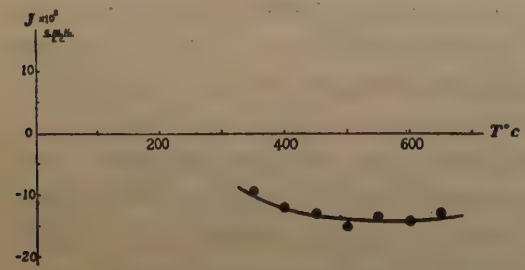


Fig. 4. Thermo-remanent magnetization, $J^{10}_{T,H=0.5}$ of the separated ferromagnetic minerals,

magnetism" or briefly **"Reverse T.R.M."**

The result shown in Fig. 3 will give us a distinct and direct evidence for the existence of the phenomenon of self-reversal of thermo-remanent magnetism of rocks.

On the other hand, T.R.M. of ensemble of ferromagnetic minerals separated from the rock is given in Fig. 4.

In the case of Fig. 4, T.R.M.s produced by cooling from a temperature above 300°C in magnitic field of 0.5 *Oe.* are always Reverse T.R.M.

Since the content of the ferromagneic minerals in their mother rocks is less than 2% in volume and those minerals grains are distributed fairly uniformly in the other non-ferromagnetic minerals, and further since the phenomenon of Reverse T.R.M. appears both in the rock samples themselves and ensemble of ferromagnetic grains separated from their mother rocks, we can conclude that the Reverse T.R.M. is principally a magnetic character of each grain of ferromagnetic minerals. In other words, the self-reversal of T.R.M. in the present case ought to be due to some inner magnetic constitution of the ferromagnetic mineral.

For the purpose of examining the above conclusion more directly, T.R.M. of special test samples, in which the contents of the concerning ferromagnetic minerals were diluted by adding a fair amount of magnetia were measured. The results showed that Reverse T.R.M.s take place in these samples regardless of the amount of content of the ferromagnetic minerals, so far as the temperature, from which the samples are cooled in a magnetic field, exceeds 300°C.

Then, magnetic behaviours of ensembles of the ferromagnetic grains will be dealt with especially in detail in the following paragraphs for the purpose of examining the characteristics of the particular phenomenon of Reverse T.R.M.

4. *Characteristics of Reverse Thermo-Remanent Magnetism of the Ferromagnetic Minerals.*

The relation of the partial thermo-remanent magnetism (P.T.R.M.) of the ferromagnetic minerals to the temperature range for partial magnetic field cooling is illustrated in Fig. 5.

The definition of partial thermo-remanent magnetism (6) is the following: During the process of cooling of sample from a temperature higher than the hightest Curie point, magnetic field H is applied on the sample only during a certain temperature range from T_{n+1} to T_n (where $T_{n+1} > T_n$), the external magnetic field being kept zero in the other temperature ranges.

The sample after thus cooled down to the room temperature maintaines a remanent magnetism, which is

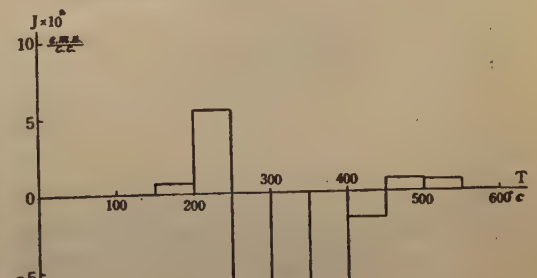


Fig. 5. P.T.R.M. $J^{T_n}_{T_{n+1},\,H=2.0}$ ($T_{n+1}-T_n=$ 50°C), of the separated ferromagnetic minerals.

called the partial thermo-remanent magnetism, and denoted by $J^{Tn}_{Tn+1,H}$. In the experiment given in Fig. 5. the temperature range $\Delta T = T_{n+1} - T_n$ was kept 50 degrees and the intensity of external magnetic field applied during the temperature range was always 2.0 *Oe.*

In the ordinary rock samles or ordinary ferromagnetic minerals, $J^{Tn}_{Tn+1,H}$ is always "positive." Such the positive partial thermo-remanent magnetization will be called "**normal partial thermo-remanent magnetism,**" or shortly **normal P.T.R.M.**

In the case shown in Fig. 5, $J^{Tn}_{Tn+1,H}$ is positive when $T_{n+1} \leq 250°C$ and when $T_n \geq 450°C$, i.e. it is N.P.T.R.M. but it is distinctly negative during the temperature range from $T_n > 250°C$ to $T_{n+1} < 450°C$. The latter case where the direction of P.T.R.M. is opposite to that of H will be named hereafter "**reverse partical thermo-remanent magnetism,**" or shortly "**Reverse P.T.R.M.**"

P.T.R.M. in the magnetic field of 0.5 *Oe.* was also measured, the results being shown in Fig. 6. The general tendency of the relation between P.T.R.M. and the temperature range of magnetic field cooling in the present case is similar to that in the case shown in Fig. 5.

On the other hand, it was proved experimentally that the above-mentioned relation of Reverse P.T.R.M. to the temperature range depends on the intensity of applied magnetic field. P.T.R.M. produced by cooling from 350°C to 250°C in various magnetic fields is shown in Fig. 7, where it is noticed that P.T.R.M. is reverse provided that the magmetic field H is less than 7.0 *Oe.*, while it becomes normal if H exceeds 7.0 *Oe.*

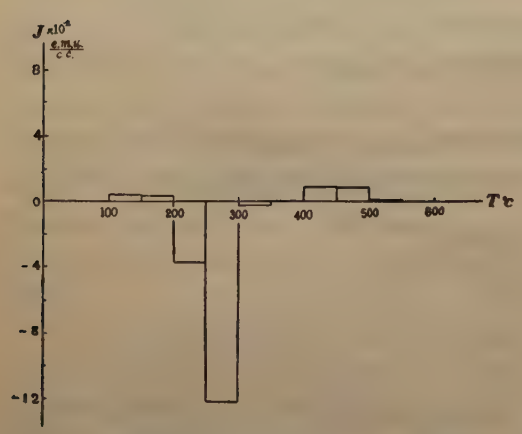


Fig. 6. P.T.R.M., $J^{Tn}_{Tn+1,H=2.0}$ ($T_{n+1} - T_n = 50°C$), of the separated ferromagnetic minerals.

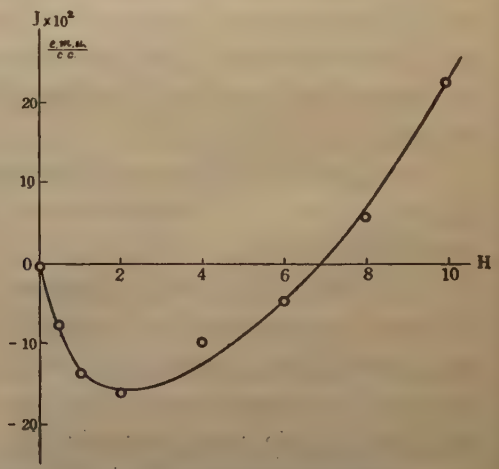


Fig. 6. Relation of P.T.R.M., $J^{250}_{350,H}$ (10°C) to the applied magnetic field H.

It seems further that the intensity of Reverse P.T.R.M. increases with the increase up to 1.5 *Oe.* of H, i.e. $\delta J/\delta H < 0$ so far as $H \lesssim 1.5$ *Oe.*, but $\delta J/\delta H > 0$ when $H \gtrsim 1.5$ *Oe.*

Thus, it may be concluded that the appearance of reversal of P.T.R.M. depends on both temperature and magnetic field.

5. *Temperature Coefficient of R.T.R.M. around the Ordinary Atmospheric Temperature.*

As is discussed in the later paragraph, the temperature cofficient of R.T.R.M. thus produced will be a significant element which is related to the constitution of this peculiar remanent magnetization.

The change of the intensity of T.R.M. with temperature in a non-magnetic space was observed by means of a ballistic method apparatus within the temperature range from −70°C to 100°C.

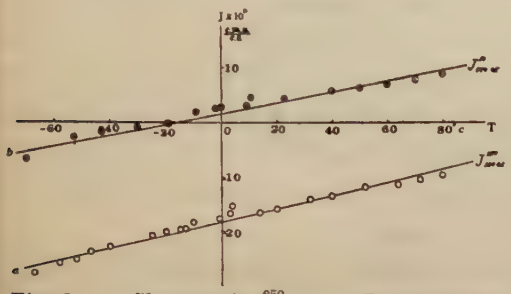


Fig. 8. a. Change of $J^{250}_{350,H=0.5}(T)$ around the room temperature.
b. Change of $J^{10}_{550,H=0.5}(T)$ around the room temperature.

The results of measurements are illustrated in Fig. 8, where curve (a) shows $J^{250}_{350,H=0.2}$ of the fresh ferromagnetic mineral, while curve (b) $J^{10}_{550,H=0.5}$ of the minearals which were once heated up to 800°C, the original mineral constitution being somewhat altered. The thermal changes shown here are reversible at least during the range of temperature from −70°C to 80°C, and the temperature coefficient is a positive constant in the said temperature renge. An interesting fact given by curve (b) is that the thermo-remanent magnetism which is apparently normal at the room temperature becomes reverse below −15°C.

Generally speaking, P.T.R.M. is a function of temperature T. Then, we can conclude in the above cases that

$$\frac{\partial}{\partial T} J^{T_1}_{T_2}(T) > 0 \qquad (1)$$

regardless of the sign of $J^{T_1}_{T_2,H}$ at the room temperature, so far as concerning the reversible thermal-change of $J^{T_1}_{T_2,H}$, where the temperature change $T_2 \sim T_1$ includes the range for reverse P.T.R.M. shown in Fig. 5.

On the the other hand, Fig 9 shows the reversible thermal changes of $J^{100}_{200,H=0.5}$ and $J^{500}_{600,H=0.5}$, where it must be noticed that these two cases were especially examined as the representatives of the parts of N.P.T.R.M. below 250°C and above 450°C respectively in Fig. 5 and that the magnetizations are normal at the room temperature.

As is shown in the figure, the temperature coefficients of those magnetizations are a little nagative,

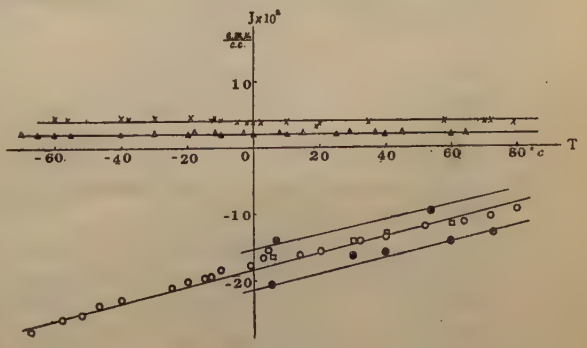


Fig. 9.

× Change of $J^{500}_{600,H=0.5}(T)$ around the room temerature.
△ Change of $J^{500,100}_{600,200,H=0.5}(T)$ around the room temperature.
▲ Change of $J^{100}_{200,H=0.5}(T)$ around the room temperature.
◉ Change of $J^{250,100}_{350,200,H=0.5}(T)$ around the room temprature.
○ Change of $J^{250}_{350,H=0.5}(T)$ around the room temperature.
● Change of $J^{500,250}_{600,350,H=0.5}(T)$ around the room temperature.
□ Change of $J^{500,250,100}_{600,350,200,H=0.5}(T)$ around the room temperature.

but its absolute magnitude is far small compared with that shown in Fig. 5. In other expressions,

$$\frac{\partial}{\partial T} J^{T'_1}_{T'_2\ H}(T) \lesssim 0 \qquad T'_2 < T_{c1}$$

$$\frac{\partial}{\partial T} J^{T''_1}_{T''_2\ H}(T) \gtrsim 0 \qquad T''_1 > T_{c2} \qquad (2)$$

where T_{c1} and T_{c2} are the critical temperatnres defined in Fig. 5 and (1).

Since the thermal change of magnetization mentioned above is reversible with respect to temperature in a non-magnetic space, the magnetization concerned ought to be the sum of spontaneous magnetization of domains which are fixed by the process of magnetic field cooling. Then, we may assume that the spontaneous magnetization in the case of Fig. 8 contains a particular element quite different from that in the case of Fig. 9. In other words, it seems that the ferromagnetic mineral is composed at least of two different kinds of ferromagnetic substance.

In order to examine the composition and possible relations among the elemental magntizations the temperature coefficient of T.R.M. of the same sample treated with various combinations of the three representative processes of magnetic field cooling was measured, where the said three processes were the cooling in magnetic field of 0.5 *Oe.* from 600°C to 500°C, from 350°C to 250°C and from 200°C to 100°C. The results of experiments are shown in Table II, where, for instance, the notation $J^{500,100}_{600,200,0.5}$ means T.R.M. produced by the superposition of two processes of magnetic field cooling from 600°C to 500°C and from 200°C to 100°C in 0.5 *Oe.*

Table II

Treatment of magnetic field cooling	Intensity at 15°C	Mean temperature coefficient (−70°C∼+80°C)	Character of T.R.M.	Sign of temp. coef.
$J^{500}_{600,H=0.5}$	$+\ 3.9\times10^{-2}$ e.m.u./cc	$-\ 5\times10^{-6}$ e.m.u./cc/degree	Normal	− (small)
$J^{250}_{350,H=0.5}$	-16.7×10^{-2}	$+10.5\times20^{-4}$ e.m.u./cc/degree	Reverse	+
$J^{100}_{200,H=0.5}$	$+\ 2.1\times10^{-2}$	$-\ 2\times10^{-6}$ e.m.u./cc/degree	Normal	− (small)
$J^{500,100}_{600,200,H=0.5}$	$+\ 2.1\times10^{-2}$	$-\ 2\times10^{-6}$ e.m.u./cc/degree	Normal	− (small)
$J^{500,250}_{600,350,H=0.5}$	-20.7×10^{-2}	$+10.0\times10^{-4}$ e.m.u./cc/degree	Reverse	+
$J^{250,100}_{350,200,H=0.5}$	-14.1×10^{-2}	$+\ 9.6\times10^{-4}$ e.m.u./cc/degree	Reverse	+
$J^{500,250,100}_{600,350,200,H=0.5}$	-16.3×10^{-2}	$+10.5\times10^{-4}$ e.m.u./cc/degree	Reverse	+

From these results, the following conclusions will be obtained: (a) Any process including the magnetic field cooling of 350°C→250°C produces R.T.R.M., the temperature coefficient of which is positive and large around the room temperature. So that such the process as mentioned above will be called R-process for the sake of convenience of expression.

(b) The magnetic field cooling process of 600°C→500°C and 200°C→100°C and their superposition result in Normal T.R.M., the temperature coefficients of which is small. These processes will be named by N-1 and N-2 processes respectively.

(c) The addition law of P.T.R.M., which has been established for the case of ordinary T.R.M., does not exactly hold in the present case.

6. *Process of Development of Reverse Thermo-Remanent Magnetism.*

In order to see directly the process of development of R.T.R.M., the change in magnetization of the ferromagnetic minerals with temperature was measured by means of a ballistic method schematically illustrated in Fig. 10. The results of experiment are given in Figures 11~19 where the hollw

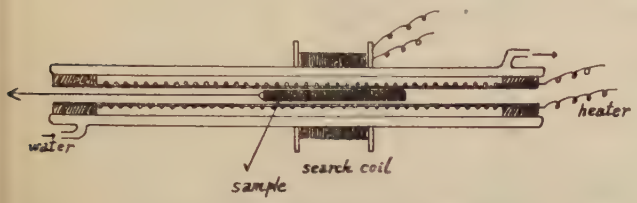


Fig. 10. Measuring apparatus for development and decay of T.R.M.



Fig. 11. Development and decay of $J^{500}_{600,\,H=0.5}(T)$

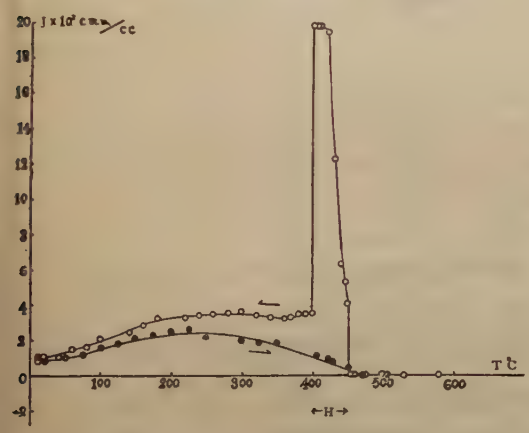


Fig. 13. Development and decay of $J^{400}_{450,\,H=0.5}(T)$

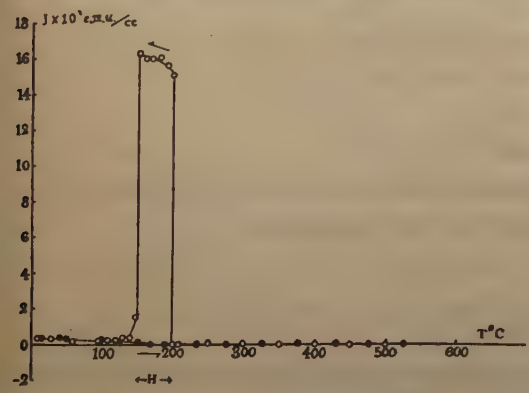


Fig. 15. Development and decay of $J^{300}_{350,\,H=0.5}(T)$

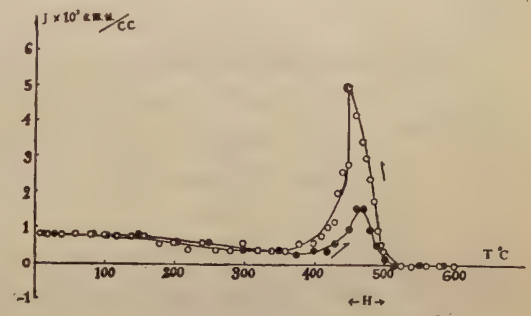


Fig. 12. Development and decay of $J^{450}_{500,\,H=0.5}(T)$

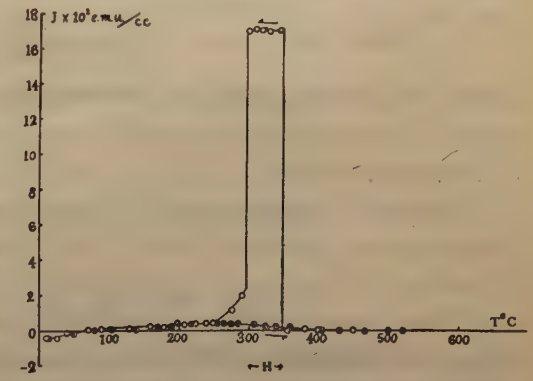


Fig. 14. Development and pecay of $J^{350}_{400,\,H=0.5}(T)$

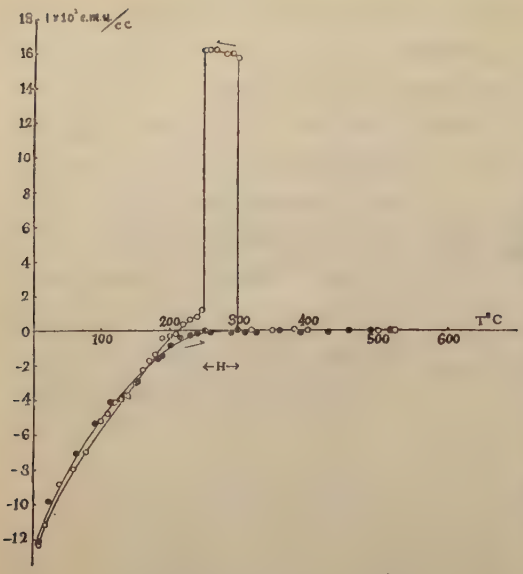


Fig. 16. Development and decay of $J^{250}_{300,H=0.5}(T)$

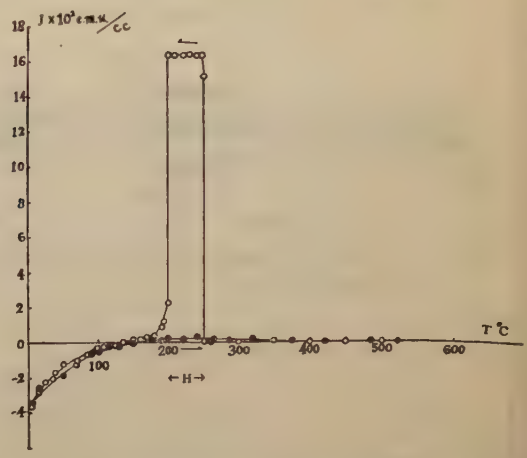


Fig. 17. Development and decay of $J^{200}_{250,H=0.5}(T)$

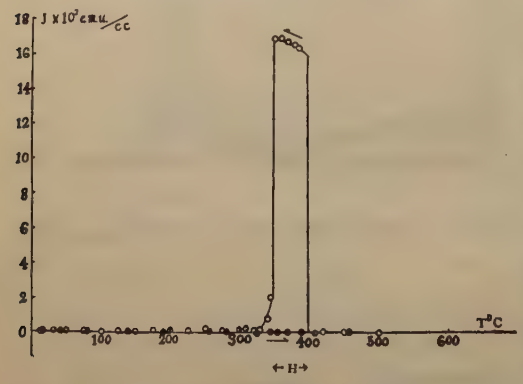


Fig. 18. Development and decay of $J^{150}_{200,H=0.5}(T)$

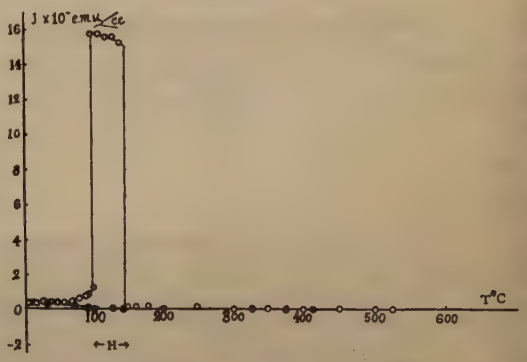


Fig. 19. Develompment and decay of $J^{100}_{150,H=0.5}(T)$

circles show the magnetization in the cooling process (the process of development of P.T.R.M.), while the full circles the re-heating process (the process of disappearance of P.T.R.M.).

Here, the magnetization at a temperature T between T_1 and T_2 in the cooling process can be given by

$$J(T)=J_r(T)+J^r_{T_2H}(T), \qquad T_1<T<T_2, \tag{3}$$

where $J_r(T)$ means the reversible part of magnetization, being almost proportional to H so far as H is small: while when $T<T_1$ in the coolinig process

$$J(T)=J^r_{T_2H}(T) \qquad T<T_1 \tag{4}$$

since no external magnetic field is applied below T_1.

That is, throughout all examples shown in the figures, the discontinuous rise in magnetization in the temperature range (T_1, T_2) in the cooling process is due to the

addition of the reversible magnetization J_r.

In the re-heating process without magnetic field, on the contrary, the measured magnetization is to be shown by

$$\begin{aligned} J(T) &= J^{T_1}_{T_2,H}(T) && T<T_1 \\ &= J^{T}_{T_2,H}(T) && T_1<T<T_2 \\ &= 0 && T_2<T \end{aligned} \qquad (5)$$

In the series of Figures 11~19, the changes with temperature of $J^{600}_{600}(T)$, $J^{450}_{600}(T)$, $J^{400}_{450}(T)$, $J^{350}_{400}(T)$, $J^{300}_{350}(T)$, $J^{350}_{300}(T)$, $J^{200}_{250}(T)$, $J^{150}_{200}(T)$ and $J^{100}_{150}(T)$ are illustrated successively.

The suffix concerning H in the notation of $J^{T_1}_{T_2,H}(T)$ will be omitted hereafter, since the magnitude of H is kept constant throughout all experiments dealt with in this paragraph, i.e. $H=0.5$ *Oersteds*.

The magnitude of $J^{T_1}_{T_2,H}(T)$ in the cooling process and that in the re-heating process given in these figures show a definite amount of discrepancy. We may assume at the present stage that the said discrepancy is due to the condition that the magnetization in the cooling process contains a little after-effect of foregoing magnetization with respect to time. In other words, it seems that the magnetic domains were not perfectly fixed a little while after removal of external magnetic field in the cooling process.

$J^{600}_{600}(T)$, $J^{450}_{500}(T)$ and $J^{400}_{450}(T)$ belong to N_1-process described in § 5, and they are normal in the direction of magnetization. However, $J^{500}_{600}(T)$ and $J^{450}_{500}(T)$ rise up around 450°C both in the cooling and re-heating processes. This is a particular phenomenon, since $J^{T_1}_{T_2,H}(T)$ curve of the ordinary T.R.M. increases monotonously with decrease in temperature in accordance with the Curie's law.

$J^{400}_{450}(T)$ in Fig. 12 shows a more complicated form, the remanent magnetization decreasing with decrease in temperature below 200°C. This is also a particular case compared with the characteristics of the ordinary T.R.M.

$J^{350}_{400}(T)$ shown in Fig. 14 is a transient state between N_1-process and R-process, giving very little remanent magnetization.

On the other hand, $J^{300}_{350}(T)$, $J^{250}_{300}(T)$ and $J^{200}_{250}(T)$ belong to R-process mentioned in § 5. The most typical example of this group will be $J^{250}_{300}(T)$ shown in Fig. 16, where the remanent magnetization decreases almost linearly with decrease in temperature after the removal of external magnetic field at 250°C, and crosses the zero-line at about 200°C, becoming the reverse T.R.M. below the said critical temperature. The change in $J^{250}_{300}(T)$ with temperature is almost-reversible so far as T does not exceed 200°C. It must be recalled that the above-mentioned reversible and linear change with temperature holds in the temperature range, at least, down to −70°C.

The general tendency of the curves of $J^{300}_{350}(T)$ and $J^{200}_{250}(T)$ are the same as that of $J^{250}_{300}(T)$, though the reverse T.R.M. in the former two cases are small.

$J^{150}_{200}(T)$ and $J^{100}_{150}(T)$ given in Figures 18 and 19 are generally of the normal form, and these cases are classified into N_2-process in § 5.

It may be concluded from the above-mentioned results that the reverse T.R.M. is produced chiefly in the temperature range from 300°C to 250°C or in somewhat wider range under the effect of an external magnetic field.

Further, it must be noticed by summarizing the results given in § 5 and § 6, that the positive temperature coefficient of the reverse T.R.M. is fairly large and kept nearly constant through a fairly wide range of temperature, since this is to be a distinct contrast against the negative temperature coefficient of ordinary T.R.M. which follows the Curie's law.

It will also be worthwhile to point out that the rise up of $J_{T_2}^{T_1}(T)$ curve given by N_1-process in a certain temperature range can hardly harmonize with the ordinary conception of ferromagnetism, so far as we assume that T.R.M. is the sum of spontaneous magnetizations of the domains fixed by the process of magnetic field cooling.

7. *Process of Development of Total Thermo-Remanent Magnetization in the Case where Reverse P.T.R.M. is enclosed.*

In the view of geophysical standpoint, one's interest may concern the process of development of reversed total thermo-rement magnetization which is produced by cooling from a certain high temperature throughly in a magnetic field. Hence, the above-mentioned process was measured by the apparatus described in the preceding paragraph. Fig. 20 shows an example of measurements, where H was kept 0.5 *Oe.* throughout the whole process of cooling. In this figure, the change in magnetization with temperature is also shown in the case of initial heating of the same sample in the same magnetic field, where the sample had been thermally demagnetized before the measurement. Following the notations given in § 6, the intensity of magnetization in the initial heating process is given by

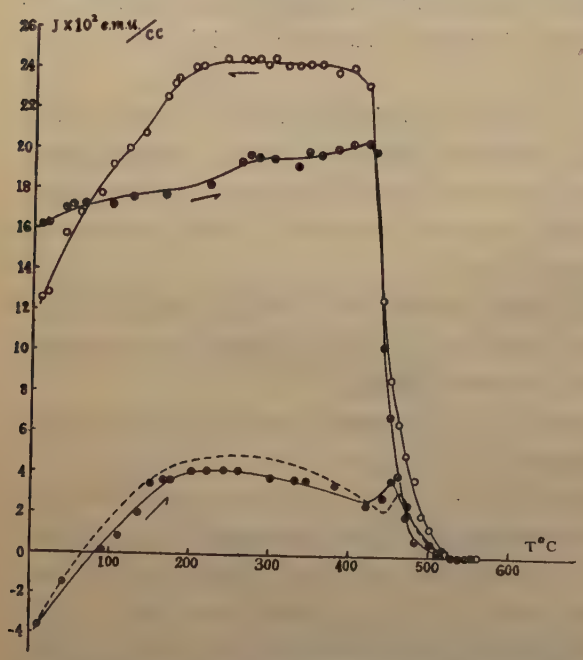


Fig. 20. Change in total magnetization of the sample with temperature.

A. double dircles : magnetization in the process of heationg in $H=0.5$ *Oe.*

B. hollow circles : magnetization in the process of cooling in $H=0{\cdot}5$ *Oe.*

C. full circles : T.R.M., obtained by B-Process, in the process of heating in $H=0$.

D. broken lin : difference of A from B.

$$\vec{J}_h(T)=\vec{J}_r(T) \qquad (6)$$

while that in the cooling process by

$$\vec{J}_c(T)=\vec{J}_r(T)+\vec{J}_{\theta H}^{T}(T) \qquad (7)$$

where θ denotes the Curie point temperature. It will be expected therefore that the difference

between the $J_c(T)$ curve and the $J_h(T)$ curve at a same temperature in Fig. 20 is shown by

$$\vec{J}_c(T)-\vec{J}_h(T)=\vec{J}^{T}_{\theta H}(T) \qquad (8)$$

The difference $J_c(T)-J_h(T)$ thus derived is also shown in Fig. 20 by the borken line curve which becomes negative below 85°C.

After the removal of H at room temperature (10°C), the sample has a negative remanent magnetization, i.e. Reverse T.R.M., as already described in § 3. And the intensity of the Reverse T.R.M. is just coincident with the magnitude of $J_c(10°C)-J_h$ (10°C).

The sample thus treated was again heated in a non-magnetic space, the change of T.R.M. in this case being shown by full circles in Fig. 20. The magnetization in this case is to be equal to $\vec{J}^{T}_{\theta H}(T)$, provided that T.R.M. is assumed to be caused by fixing a certain part of magnetic domains by the magnetic field cooling. It will be seen in the figure that $\vec{J}^{T}_{\theta H}(T)$ thus directly measured is almost equal to $J_c(T)-J_h(T)$ at any temperature. This fact may indicate that the relation given by (8) and consequently that given by (7) holds fairly well in the present case.

8. *Possible Mechanism of Causation of Reverse Thermo-Remanent Magnetization.*

It will be concluded from the experimental results that Reverse T.R.M. is a definite physical phenomenon, reproducible and universal, provided that certain physical conditions are fulfilled in the ferromognetic grains. There will be a few theoretical possibilities of self-reversal of thermo-remanent magnetization, as already been pointed out by L. Néel (10). Those possibilities may belong to two different categories.

The first one is that the ferromagnetic mineral sample contains more than two different constituents which have an intense magnetic interaction to each other, so that one of them is magnetized by the demagnetizing field of another which has been magnetized by the external field, the remanent magnetization of the former bringing about Reverse T.R.M. according as the specimen is cooled.

The other case is the ferrimagnetic substance, spontaneous magnetization of which belongs to *N*- or *V*-type according to Néel's classification (13).

It does not seem that our experimental results obtained so far are enough sufficient to allow one to determine finally which one of these mechanisms should be the real. The following discussions are to treat this problem briefly on the basis of the experimental results, where are used the notations that

T_b domain fixing temperature,
H intensity of external magnetic field,
J_i irreversible or fixed magnetization,
J_r reversible magnetization,
σ intensity of spontaneous magnetization,
n number of fixed magnetic domains per unit volume,
v volume of a magnetic domain.

The capital letters such as *A*, *B*, and *C* represent the ferromagnetic constituents

involved.

One may notice from Figs. 11, 12, 13, 18 and 19, that the magnetizations produced in N_1 and N_2 processes are not playing any essential role in the formation of Reverse T.R.M., although the abrupt increase of magnetization at about 450°C in Figs. 12 and 20 will be an interesting fact. Therefore the domain fixing temperatures of the constituents essential to Reverse T.R.M. must be in the comparatively narrow range, i.e. the range where the R-process takes place.

1) *Reverse T.R.M. as a result of magnetic interaction between different constituents.*

The first type of the theoretical possibilities is based upon following assumptions. The sample contains two different ferromagnetics A and B having different domain fixing temperatures ${T_b}^A$ and ${T_b}^B$ and the magnetic domains of A are fixed at ${T_b}^A$ in the direction of H during the process of cooling in H, resulting in an irreversible magnetization as follows.

$$ {J_i}^A(T)=n_A\cdot v_A\cdot\sigma_A(T), \quad \text{where} \quad T\leq {T_b}^A. \tag{9} $$

Then the effective field H_{eff} on the domains of B at $T={T_b}^B$ becomes

$$ H_{eff}=H-\{D\cdot J_r({T_b}^B)+\alpha\cdot {J_i}^A({T_b}^B)+\beta\cdot {J_i}^B({T_b}^B)\} \tag{10} $$

where D, α, and β are some constants representing demagnetizing factors. If ${J_i}^A(T)$ increases as much as to make H_{eff} in (10) negative, the total irreversible magnetization at $T<{T_b}^B$ becomes

$$ J_i(T)={J_i}^A(T)+{J_i}^B(T)=n_A\cdot v_A\cdot\sigma_A(T)-n_B\cdot v_B\cdot\sigma_B(T) \tag{11} $$

Hence, if the condition

$$ \frac{n_A\cdot v_A}{n_B\cdot v_B}<\frac{\sigma_B(T)}{\sigma_A(T)} \tag{12} $$

holds, the resultant magnetization can be negative. Moreover, since $J_i(T)$ in (11) is, theoretically or experimentally, positive at ${T_b}^B$, the condition to make it negative at room temperature becomes

$$ \frac{\sigma_A(T)}{\sigma_A({T_b}^B)}<\frac{\sigma_B(T)}{\sigma_B({T_b}^B)}. \tag{13} $$

This condition seems plausible from our experimental result that the temperature coefficient of $J_i(T)$ produced in R-process is large. Thus, if $\sigma_B(T)$ increases enough steeply, $J_i(T)$ at the room temperature can be Reverse T.R.M..

There are several ways in interpreting the possible machanism of the magnetic interaction between the two constituents assumed above. For instance, in the Néel's model the interaction is supposed to act between the grains of different constituents A and B, assuming that the grains of A and B are of the form of prolate ellipsoid and mixed homogeneously with concentration of c_A and c_B. Then $J^{T_1}_{T_2,H}(T)$, where $T<T_1$, is expressed as,

$$ J^{T_1}_{T_2,H}(T)=H\left\{\frac{\sigma_s{}^B(T)}{\sigma_s{}^B({T_b}^B)}\frac{c_B{s_b}^B\{1-2(c_A+c_B)\}-c_A d{s_b}^A\dfrac{\sigma_s{}^A({T_b}^B)(1-2c_A)}{\sigma_s{}^A({T_b}^A)\left(1-\frac{2}{3}c_A\right)+{s_b}^A c_A d}}{\left\{1-\frac{2}{3}(c_A+c_B)\right\}+c_B d{s_b}^B}+c_A{s_b}^A\frac{\sigma_s{}^A(T)}{\sigma_s{}^B({T_b}^A)}\frac{1-2c_A}{\left(1-\frac{2}{3}c_A\right)+c_A d{s_b}^A}\right\} \tag{14} $$

where d and s denote the difference in demagnetizing factors of sphere and the ellipsoid in the direction of long axis and the susceptibility as to the irreversible magnetization at T_b. In (14), the first and second terms correspond to the irreversible magnetization of B and A, and condition for appearance of Reverse T.R.M. is,

$$J^{T_1}_{T_2,H}(T)<0, \qquad T\ldots\text{.room temperature.} \tag{15}$$

Néel derived a more explicit formula from (14) by using a simpler model and shown that the occurence of Reverse T.R.M. is not impossible provided that proper values are assumed for the quantities involved in the equation.

The above mentioned Néel's model seems to be consistent in itself and actually probable. This model, however, does not seem to be applied for the explanation of our experimental results: if the above theory is accepted, P.T.R.M., $J^{T_1}_{T_2,H}(T)$, where $T_1<T_b{}^B<T_2<T_b{}^A$, must be in the normal direction and have a large temperature coefficient which is minus in sign, because in this model the observed large positive coefficient of Reverse T.R.M. is to be caused by the steep development of $\sigma_B(T)$ with decrease in temperature. But no such the result has ever been obtained. Another example unfavorable to this machanism will be that the re-heating curves of irreversible magnetization produced by R-process hardly exceed the zero line, for this tendency makes it quite dubious that there were such an intense normal remanent magnetization at $T_b{}^B$ as to magnetize B in the reverse direction by its demagnetizing field in the cooling process.

In the present paper, we shall tentatively attack another possibility. The above facts and another that Reverse T.R.M. is fairly stable, changing reversibly with temperature below T_1, may suggest that the whole process of fixing of domains in reverse direction takes place during the cooling from T_2 and T_1. If so, the domains in question must be orientated into the reverse direction while the extertal magnetic field magnetizes the total magnetization, including the reversible part of it, in the normal direction. Examing $J(T)$-T curves in Figs. 16 and 17, for example, we can observe the fact that the reversible part of magnetization is markedly large. This means that the reversible part should be the major factor in producing the demagnetizing field.

Now we shall assume a somewhat modified model, where the sample is composed also of constituents A and B. Constituent A is the main constituent of this sample and is supposed to be the same with the normal ferromagnetic minerals. $\sigma(T)$ in Fig. 2 would be the spontaneous magnetization of A. The magnetization of A is composed of two parts as is in the other ordinary specimens, i.e. the reversible part r and the irreversible part C. The domain fixing temperature of constituent B is to be in the R-temperature range and $\sigma_s{}^B(T)$ incerases so steeply as to cause the large temperature coefficient of $J^{T_1}_{T_2,H}(T)$ observed. B is assumed to be in a peculiarly close magnetic coupling with r. The content of B is scanty compared with that of A. Therefore $J_i{}^B$ is easily saturated while J_r and $J_i{}^C$ increase with the increase of H. In the remanent magnetization by stronger field, $J_i{}^C$ begins to play the major role.

According to the model described above, let us investigate $J_{T_2,H}^{T_1}$ produced in R-process, i.e. $T_1<T_b{}^B<T_2$. Magnetization is expressed in general as,

$$J(T)=J_i(T)+J_r(T). \tag{16}$$

When H is weak, the equation (16) becomes,

$$J(T)=J_r(T)+J_i{}^C(T)=n_r(T)\cdot\sigma_r(T)\cdot v_r\cdot H+J_i{}^C(T), \quad \text{where} \quad T_b{}^B<T<T_2 \tag{17}$$

$$\begin{aligned}J(T)&=J_r(T)+J_i{}^B(T)+J_i{}^C(T)\\&=n_r(T)\cdot\sigma_r(T)\cdot v_r\cdot H+n_i{}^B(T_b{}^B)\cdot\sigma_B(T)\cdot v_B\{H-D_{Br}\cdot J_r(T_b{}^B)\}+J_i{}^C(T)\\&\qquad \text{where} \quad T_1<T<T_b{}^B\end{aligned} \tag{18}$$

$$\begin{aligned}J(T)&=J_i{}^B(T)+J_i{}^C(T)=n_i{}^B(T_b{}^B)\cdot\sigma_B(T)\cdot v^B\{H-D_{Br}\cdot J_r(T_b{}^B)\}+J_i{}^C(T)\\&\qquad \text{where} \quad T<T_1.\end{aligned} \tag{19}$$

In these equations n denotes the number of magnetic domains, in a unit volume, susceptible to a unit magnetic field and D_{Br} represents the demagnetizing factor of $J_r(T)$ affecting on B. If one puts $J_r(T)=0$ in the above equations, the expressions for the re-heating curves are to be obtained. Hence, as long as $J_i{}^C(T)$ is small, the tendency that re-heating curves do not exceed the zero line can be explained, and the necessary condition for Reverse T.R.M. is

$$H-D_{Br}\cdot J_r(T_b{}^B)<0. \tag{20}$$

In this model, the essential problem is how such an intense magnetic interaction can be possible. The macroscopic model as Néel's is not applicable in our case, because the concentration of ferromagnetic grains does not affect the magnitude of Reverse T.R.M. Such a close magnetic interaction should be, in the authors' opinion, of the domain scale.

When H is strong, the magnitude of $J_i{}^C(T)$ increases and the reheating curves begin to exceed the zero line and at last $J_i(T)$ at room temperature becomes normal.

2) *A model containing N- or V-type ferrimagnetic substance.*

As has been mentioned in the beginning of this paragraph, another almost equally probable mechanism may be established if the existence of N- or V-type ferrimagnetic constituent (7) in the present sample is assumed. The mode of thermal change in spontaneous magnetization of N-type is shown in Fig. 21. If the domain fixing temperature of this constituent, T_b, which is in our example supposed to be in R-process temperature range, exists in the temperature range between Θ_p and Θ_c in Fig. 21, Reverse T.R.M. may be expressed as follows,

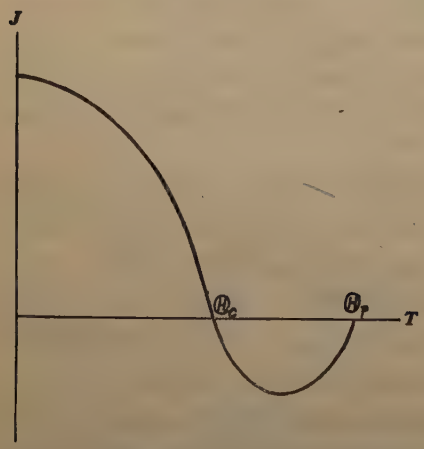


Fig. 21. Change with temperature of spontaneous magnetization of N-type ferrimagenetism.

$$J_{T_2,H}^{T_1}(T)=n(T_b)\cdot\sigma(T)\cdot v\cdot H, \quad \text{where} \quad T_1<T_b<T_2 \quad \Theta_c<T_b<\Theta_p \quad T<T_1 \tag{21}$$

In such a model it is obvious that the particular nature of $\sigma(T)$ would make $J_{T_2,H}^{T_1}(T)$

negative below Θ_c. This model, however, is obliged to have the same difficulty with the model containing two fixing constituents in explaining the observed distinct tendency that the re-heating curves in Figs. 16 and 17 hardly exceed the zero line.

9. *Conclusion and Further Problems.*

It seems that the existence of self-reversal of thermo-remanent magnetism in nature was proved by the present study, and that Reverse T.R.M. can be attributed to the magnetic characteristics of ferromagnetic (or ferrimagnetic) mineral grains.

Physical mechanism of causation of this particular phenomenon, however, has not yet been fully clarified, though several facts directly connected to the mechanism were obtained in the present experiments. The problem of Reverse T.R.M. will be significant from two different standpoints of view, one being in connection with geophysical problem, especially with palaeomagnetism, while the other is with physics of magnetism, especially with characteristics of ferrimagnetic substances.

From the standpoint of geophysics, it will be desirable that a large number of igneous rocks which have reverse remanent magnetization *in situ* are examined in the same way as here. Studies of some of other Japanese samples are now under going. But it will be further desirable that the rook samples collected from various localities over the world are examined by a systematic method.

From the standpoint of physical study of "ferrite" substances, the mechanism of development of Reverse T.R.M. will be especially interesting, since the phenomenon looks like closely relating to Néel's ferrimagnetism. The best way will be to separate out the component of the mineral grains which are directly responsible for Reverse T.R.M., and to study various physical characteristics of that component. Another problem will be the behavior of Reverse T.R.M. at lower temperatures. The study of the latter problem is now under working.

In concluding, the writers wish to express their sincere thanks to Dr. H. Kuno and Dr. I. Iwasaki for their kind cooperation in petrological and chemical works respectively in the present study. Their hearty thanks are also due to Prof. L. Néel for his valuable dicussions in the course of this study, and to Prof. S. Nakamura and Prof. M. Hasegawa for their interest and encouragement.

References

(1) M. Matuyama, Proc. Imp. Acad. of Japan, **5**, 203 (1929)
(2) F.G. Bruckshaw and E.I. Robertson, M.N.R.A.S. Geophys. Suppl., **5**, 308 (1949)
(3) A. Roche, C.R. Ac. Sc., **233**, 1132 (1951)
(4) J.G. Königsberger, Terr. Mag., **43**, 119–130, 299–320 (1938)
(5) E. Thellier, Ann. Inst. Phys. Globe., **16**, 157 (1938)
(6) T. Nagata, Bull. Earthq. Res. Inst., **21**, 1 (1943)
(7) L. Néel, Ann. de Geophys., **5**, 99 (1949)
(8) R. Chevallier, Ann. de Physique, **4**, 5 (1925)

(9) N. Kumagai, N. Kawai and T. Nagata, Journ. Geomag. Geoel., **2**, 61 (1950)
(10) L. Néel, Ann. de Geophys., **7**, 90 (1951)
(11) I. Iwasaki and K. Katura, Kyûsyû Kôzan Gakukai-si, **18**, 201 (1950)
(12) S. Akimoto, Journ. Geomag. Geoel., **3**, 47 (1951)
(13) L. Néel, Ann. de Physique, **3**, 137 (1948)

The Meeting of the Society of Terrestrial Magnetism and Electricity:

The 11th General Meeting was held at Tokyo University on April 26-28, 1952. 52 Reports were read, about 100 Members assembled.

The Tanakadate-Prize were awarded for the following excellent workers.

The 8th, Mr. N. Fukushima, at the 8th General Meeting:
On Disturbances of the Ionosphere and Terrestrial Magnetism.

The 9th, Mr. Y. Nakata, at the 8th General Meeting:
Special Observations of the Ionosphere.

The 10th, Mr. S. Utashiro, at the 8th General Meeting:
Investigations of the Magnetic Storm by the Induction Magnetograph.

The 11th, Mr. M. Goto and Mr. K. Tao, at the 10th General Meeting:
Theoretical Studies on the Propagation of VHF-Waves.

LETTER TO THE EDITORS

Semi-Diurnal Lunar Variations in the Sporadic-*E*

The critical penetrating frequency of the sporadic-*E*, *fEs*, observed at Kokubunji (139°29.3′E, 35°42.4′N) was analyzed for 12 months of June solstices in 1949–51 to obtain the semi-diurnal lunar variations in the sporadic-*E*. For the purpose of eliminating the solar variations, difference (ΔfEs) between hourly value of *fEs* and corresponding monthly median value was calculated. And, they were arranged in lunar time, reckoned from upper transit, on one sheet during 29 days [1] after the epoch of the full and the new moon, and their mean values were obtained. Same treatments were also conducted for $200\Delta fEs/\text{median}fEs$ [2].

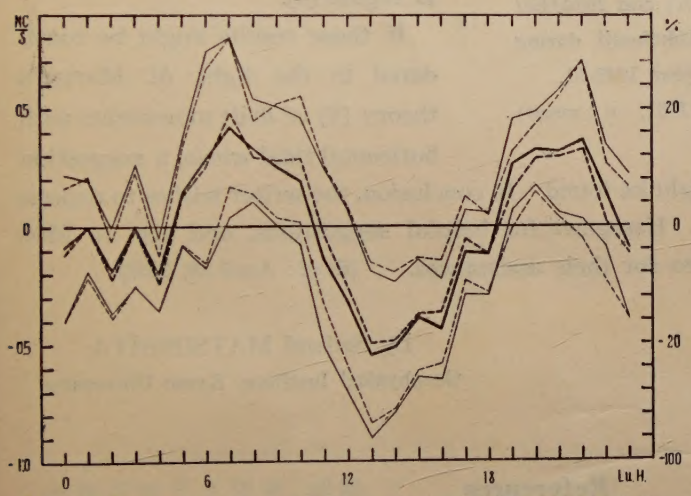


Fig. 1 Average lunar variation curves of ΔfEs (thick full-line) and $200\,\Delta fEs/\text{median}\,fEs$ (thick dotted-line) at Kokubunji during summer months for the year 1949–51. Almost all errors are contained in the band between the two thin lines. (confidence limit,95.5%)

Fig. 1 is the mean diurnal curves of 9 mean lunar variations for ΔfEs and $200\,\Delta fEs/\text{median}\,fEs$ obtained from these treatments. The semi-diurnal variations will be obvious in the figure.

A more accurate study is provided by harmonic analysis of these variations. Reliable nine results, by the analysis of the statistical significance [3], are shown by harmonic dials in Fig. 2. (Both G- and E-symbols in *fEs* data are assumed to be 0 and 0.9 MC/S, and mean values of the results for these two cases are plotted in the figure.) On the average, the lunar semi-diurnal variation attains its maximum amplitude of about 0.35 MC/S and of about 13% for $200\Delta fEs/\text{median}fEs$, approximately 8 hours after the lunar culminations.

The amplitude of the diurnal variation is generally smaller than the semi-diurnal, and the phase distributes in all quadrants of the harmonic dial. The lunar variation in December solstice and equinoxes is difficult to obtain, because of few occurrence of *Es*.

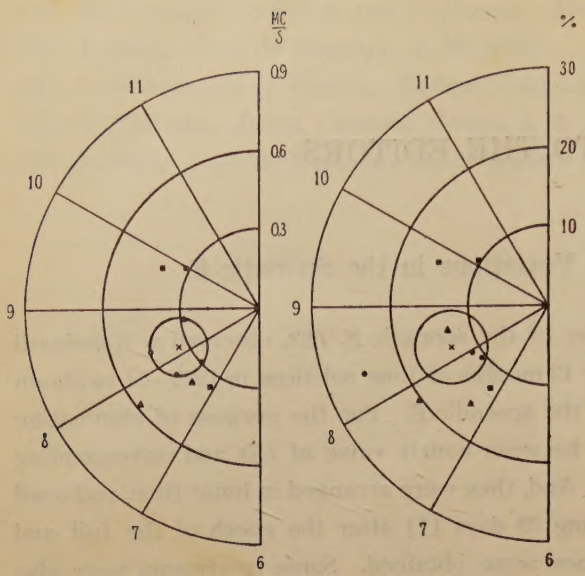


Fig. 2 Harmonic dials of semi-diurnal lunar variation in the *Es* for ΔfEs (left) and $200\Delta fEs/\text{median}fEs$ (right) at Kokubunji during summer months for the year 1949–51. (■ : 1949, ▲ : 1950, ● : 1951, × : mean)

Though the individual values of *fEs* data may have not enough accuracy to enable one to draw any tidal oscillation, the results of the above statistical study might be considered as giving some information on the semi-diurnal lunar tide in the *Es* region.

It will be attractive that the amplitude of the lunar 12 hours variation in the *Es* is much larger than that in the *E* and even in the *F2* [4], and that the phase is resemble to the *F2*, though it is different from the phase of the lunar variation of the absorption in the *D* region [5].

If these results might be considered in the light of Martyn's theory [6] of drift movements with horizontal tidal winds, a suggestion for the formation of the *Es* might be found. In conclusion, the writer wishes to express his sincere thanks to Prof. M. Hasegawa for helpful suggestions, and also to Miss M. Kato and Miss T. Nakamura for their assistances. (Read : April 28, 1952)

By Sadami MATSUSHITA
Geophysical Institute, Kyoto University

References

[1] S. Chapman & J. Bartels, Geomagnetism, Oxford, (1940).
[2] D.F. Martyn, Proc. Roy. Soc. A, **190**, 273 (1947).
[3] K. Maeda & M. Izaki, J. Geomag. Geoelect., **3**, 1 (1951); S. Chapman & J. Bartels, Geomagnetism, Oxford, (1940).
[4] D.F. Martyn, Nature, **163**, 34 (1949); Special Report on Tidal Phenomena in the Ionosphere, U.R.S.I., 1950; S. Matsushita, Rep. Ionos. Res. Japan, **4**, 57 (1950).
[5] E.V. Appleton, Nature, **164**, 308 (1949).
[6] D.F. Martyn, Proc. Roy. Soc. A, **189**, 241 (1947); Rep. Mixed Commission Ionos, I.C.S.U., 1950, 44 (1951).

昭和27年7月15日　印刷
昭和27年7月20日　發行
第4卷第1號　定價150圓
（國外定價180圓）

編輯兼發行者　日本地球電氣磁氣學會
代表者　長谷川万吉

印刷者　京都市下京區上鳥羽學校前
田中幾治郎

賣捌所　丸善株式會社京都支店
丸善株式會社　東京・大阪・名古屋・仙台・福岡

JOURNAL OF GEOMAGNETISM AND GEOELECTRICITY

Vol. IV No. 1

1952

CONTENTS

An Effect of the Atmospheric Electric Field upon the Observation of Ions in the Atmosphere, ... G. ISHIKAWA, M. KADENA and M. KITAMURA 1

A Theory of Diurnal Magnetic Variations in Equatorial Regions and Conductivity of the Ionosphere *E* Region,..... M. HIRONO 7

Self-Reversal of Thermo-Remanent Magnetism of Igneous Rocks, ... T. NAGATA, S. UYEDA and S. AKIMOTO 22

LETTER TO THE EDITORS:

Semi-Diurnal Lunar Variations in the Sporadic-*E*, ... S. MATSUSHITA 39